SafeWind

Collaborative project funded by the European Commission
under the 7th Framework Program, Theme 2007-2.3.2: Energy

"Multi-scale data assimilation, advanced wind modelling & forecasting with emphasis to extreme weather situations for a safe large-scale wind power integration"

Grant Agreement N°: 213740

Deliverable Dp-7.5

"Determination of Vref using meteorological model outputs"

DOCUMENT TYPE	Deliverable
DOCUMENT NAME:	swind deliverable_Dp7.5-Vref_v1.6.doc
VERSION:	V1.6
DATE:	2012.08.29
CLASSIFICATION:	R0: General public
STATUS:	Approved/released

Abstract: This deliverable describes methodologies for the assessment of Vref using databases from meteorological models of different resolutions in simple and complex terrain.

AUTHORS[1], REVIEWERS				
MAIN AUTHOR/EDITOR:	Xiaoli G. Larsén			
AFFILIATION:	Risø National Laboratory for Sustainable Energy, DTU			
ADDRESS:	Fredriksborgsvej 399, 4000 Roskilde, Denmark			
TEL.:	+45 2132 7332			
EMAIL:	xgal@dtu.dk			
FURTHER AUTHORS:	Elena Cantero Nouqueret (CENER), Javier Sanz Rodrigo (CENER, WPL)			
PEER REVIEWERS:	Patrick McSharry (UOXF.MQ)			
REVIEW APPROVAL:	Approved :	x	Rejected (improve as indicated below) :	
SUGGESTED IMPROVEMENTS:				
APPROVER:				

VERSION HISTORY			
VERSION[2]:	DATE:	COMMENTS, CHANGES, STATUS:	PERSON(S):
1	2011-11	First draft	X.G. Larsén
2	2012-05	New results of extreme winds in the complex terrains Navara are added.	X.G. Larsén
3	2012-06	Content about complex terrain is complete	X.G. Larsén, J. Sanz Rodrigo
4	2012-07	Final draft sent to review	X.G. Larsén, J. Sanz Rodrigo
5	2012-08	Final report reviewed	P. McSharry
6	2012-08	Reviewer's comments included and final version released	J. Sanz Rodrigo

STATUS, CONFIDENTIALITY, ACCESSIBILITY									
STATUS:				CONFIDENTIALITY:				ACCESSIBILITY:	
S0	Approved/Released	X		**R0**	General public	**X**		Private web site	
S1	Reviewed			**R1**	Restricted to project members			Public web site	**X**
S2	Pending for review			**R2**	Restricted to European Commission			Paper copy	
S3	Draft for comments			**R3**	Restricted to WP members + PL				
S4	Under preparation			**R4**	Restricted to Task members +WPL+PL				

PL: *Project leader* **WPL:** *Work package leader* **TL:** *Task leader*

[1] **The authors of this document are solely responsible for its content, which does not represent the opinion of the European Community and the European Community is not responsible for any use that might be made of data appearing therein.**

[2] **VERSION NAMING : V0.x** draft before peer-review approval, **V1.0** at the approval, **V1.x** minor revisions, **V2.0** major revision

Contents

1. Objectives 4
2. Background: methodologies for Vref Assessment 4
3. Measurements 6
3.1 Relatively simple terrain in Denmark and surroundings 6
3.2 Complex terrain Navarre region in Spain 7
4. Models and data 9
4.1 Global models and data 9
4.2 Mesoscale models 9
4.2.1 WRF 9
4.2.2 SKIRON NWP 9
4.2.3 Other models and data 10
4.3 Microscale models 10
4.3.1 WAsP 10.0 10
4.3.2 WAsP Engineering 10
5. The annual maximum method 11
6. The three methodologies 12
6.1 The selective dynamical downscaling method 12
6.2 The spectral correction method 14
6.3 The physical-statistical downscaling method using SKIRON 17
7. Results and validation 18
7.1 From the selective dynamical downscaling method 18
7.1.1 Flat terrain Denmark 18
7.1.2 Complex terrain Navara region 19
7.2 From the Physical-Statistical downscaling using SKIRON 23
7.2.1 From the measured data 23
7.2.2 From meteorological databases 24
7.2.3 Downscaling to microscale 27
7.2.4 Amplification Factor 29
7.3 From the spectral correction method 30
7.3.1 Simple terrain 30
7.3.2 Complex terrain 31
8. Discussion, Outlook 32
9. Conclusions 33
10. Acknowledgement 33
11. References 34

1. Objectives

The overall objective of this WP is to investigate several new methodologies using mesoscale and microscale downscaling for extreme wind estimation. The investigation has been done for simple terrains as well as complex terrains.

2. Background: methodologies for Vref Assessment

There are various approaches for the estimation of the extreme wind Vref. Vref, often called the T-year return wind, is a parameter that has to be estimated in order to determine which type of turbines to be used in a particular location. In the IEC 61400-1 standard (IEC, 2005), it is the 50-year return wind of 10–min values at the turbine hub height. Accurate estimate of Vref is crucial for winds not exceeding the turbine's design specification and also crucial for avoiding unrealistic over-specification.

A schematic view of Vref assessment methodologies is shown in Figure 1. The classical way is based on extreme value analysis (EVA) statistical techniques applied to historical velocity time series. EVA aims at characterizing the long term distribution of velocity maxima in order to extract the 50-year return wind from the 98% quantile. An overview of EVA methodologies for extreme winds can be found in Palutikov (1999). Regardless of the statistical method, the classical method is always limited by the short length of the observational time series, the lack of long term homogenity of the instruments or of the site conditions and, above all, the scarcity of high-quality historical observations. Furthermore, national observational networks are not maintained in the same way which brings consistency problems at trans-national level.

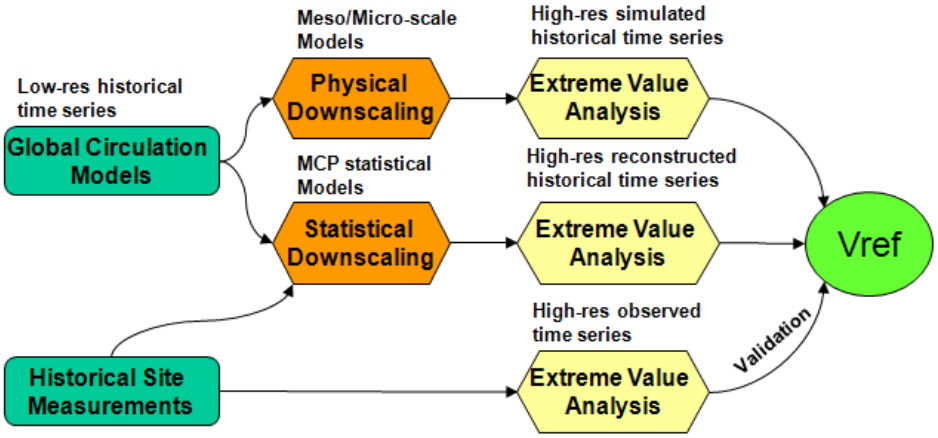

Figure 1: Sketch of Vref assessment methodologies.

This lack of long-term spatio-temporal consistency of the observational networks shall be remedied by using meteorological models. The global coverage of the input databases guaranties the spatial consistency of the meteorological model approach. Typically, reanalysis databases covering 30-50 years are produced in order to produce a homogeneous characterization of the synoptic state of the atmosphere for long term climatological studies (Kalnay et al., 1996; Dee et al., 2011). Hence, the temporal coverage and consistency is also aided by these global models.

On the other hand, global models are produced at low spatio-temporal resolution of some tens of kilometers and some hours, producing a smoothed representation of the wind climate. To overcome this limitation, downscaling methods are used in order to introduce finer scales and increase the wind speed variability typical of local scales. Two approaches can be followed: physical downscaling using mesoscale and microscale models or statistical downscaling using statistical correlation techniques together with the site measurements.

Physical downscaling uses atmospheric models forzed by global model data to dynamically introduce finer scales down to microscale level. Typically, a mesoscale model will reproduce scales of the order of 1-10km and a microscale model will be dynamically or statistically nested to the mesoscale output in order to reach spatial resolutions of the order of 100m. The physiscal downscaling method does not require the use of site measurements and, therefore, it is suitable for producing maps of wind characteristics.

Statistical downscaling is a cost-effective solution for Vref assessment if site measurements are available. The idea is to correlate the onsite short-term observational time series, which includes all the local effects, with the historical time series of the global model, which includes all the long-term climatological variability of the wind. The method is similar somehow to measure-correlate-predict (MCP) methods used in wind resource assessment for long-term extrapolation (Rogers et al, 2005). In effect, the statistical method produces a reconstruction of the historical time series that can be subsequently used by EVA techniques to extract the Vref.

Both downscaling techniques can be validated if high-quality historical observations, ideally of a duration of at least 50 years, are available. The validation process should include a variety of wind climates and site complexities in order to determine the range of applicability of the models. The existence of such network of quality observations is dubious, hence the model developer is often forced to mix databases of various sources and qualities with the inherent limitations that this implies. In this work package, we introduce three new methodologies for the extreme winds for site assessment applications. These methodologies all confront the many issues in mesoscale modelling of extreme wind events. The three new methods are described in Section 4.1, 4.2 and 4.3. The first two are developed in connection with the microscale model WEng where the annual maximum method is the statistical approach to obtain Vref. The results from the two methods can eventually be put into WEng, or some other microscale models by some adjusting, to obtain site specific extreme wind. The third method explores the possibilities of using CENER's downscaling techniques for mean wind climates in the study of extreme winds. The technique uses mesoscale modeling with SKIRON model and statistical speed-up factors from microscale modeling with WAsP (Wind Atlas Analysis and Application Program) in order to produce virtual mast data that can be post-processed in the same way as measurements.

3. Measurements

As mentioned in the previous section, long term measurements of reliable quality are very important for accurate estimation of the extreme wind. Normally they are very difficult to find, fortunately here we have access to such measurements from several places where the terrains are of various degrees of complexity. These measurements are used to examine the quality of mesoscale modelling, to validate the methodologies and to validate eventually the estimation of Vref.

3.1 Relatively simple terrain in Denmark and surroundings

The measurements include 10 min time series of quality-checked wind speed, direction, temperature and pressure. There are eight sites from Denmark, one site from Germany (FINO) and one commercial site from Sweden ('1') as presented in Figure 2. Thus there are four offshore sites and the others are in the coastal areas. The terrain in the coastal area, although rather flat, could be rather complicated because of the mixture of land and water. Some of the details of the sites and measurements regarding the measurement period, heights and data coverage are listed in Table 1. It could be noticed from Table 1 that not all measurements are long enough to be used for the extreme wind estimation (at least site 1 and Nysted). These data are however useful for testing some of the procedures in the new developed method in Section 5.1. All measurements are used for validating both two new methods developed.

In Denmark, the extreme wind mechanism is rather simple. It accompanies with the synoptic Atlantic depression systems.

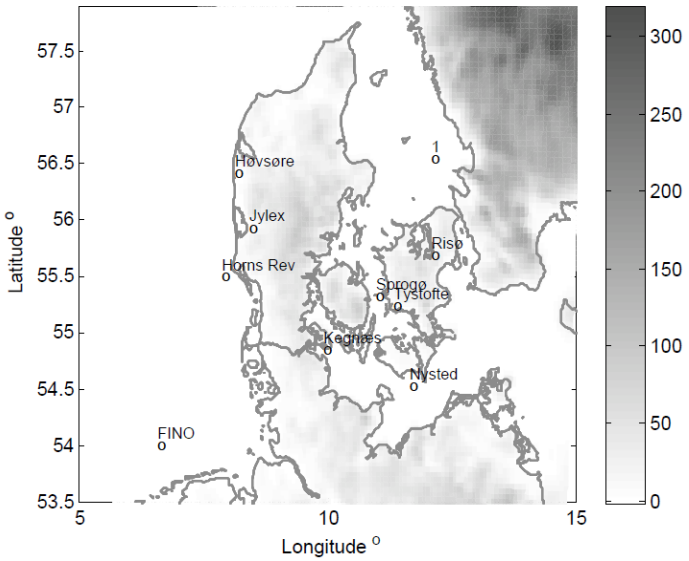

Figure 2: *Sites and locations on the elevation map over Denmark and surroundings. The elevation data are as used in the WRF simulation. (From Larsén et al. 2012b)*

Table 1: *Details of measurements for the sites in Denmark, Germany and Sweden. (*): a confidential commercial case.*

Stations	Lat. (°N)	Lon. (°E)	Data period	Height (m)	Data coverage
Sprogø	55.331	10.974	1977 - 1999	70	97.8%
Tystofte	55.24	11.33	1982 - 2010	39	96.7%
Kegnæs	54.856	9.936	1991 - 2006	23.4	99.5%
Jylex	55.942	8.449	1982 - 2004	24	96.4%
Risø	55.695	12.089	1996 - 2009	76.6	99.4%
Høvsøre	56.433	8.15	2004 - 2010	100	99.1%
Horns Rev	55.508	7.875	1999 - 2006	62	91.8%
Nysted	54.535	11.664	2004 - 2008	69	80.0%
FINO1	54.014	6.588	2004 - 2010	50	92.5%
c.s. (*)	56.561	12.105	2008 - 2010	60	99.2%

3.2 Complex terrain Navarre region in Spain

In order to analyze the use of downscaling models to estimate Vref in complex terrain, 11 10-m-high met stations with good data quality from the meteorological network of Navarre (http://meteo.navarra.es/) have been selected for this study (Figure 3, Table 2). The dataset covers the common period from the 1st of December 2003 to the 30th of November 2010. Observations of wind speed and direction were recorded at a height of 10 meters above ground level and with a time resolution of 10 minutes. Missing data periods occur randomly and have not been reconstructed because the data coverage is high.

Navarre is located in the north of the Iberian Peninsula, the orography of the region shows a variety of rich features broadly limited by two large mountain systems: the Iberic System in the South of Navarre and the Pyrenees in the North, which merge westward with the last foothills of the Cantabrian Mountains . Between them, the Ebro Valley crosses the region from northwest to southwest toward the Mediterranean. A closer look at the Navarre region reveals a complex array of smaller mountain ranges and valleys. The complexity of the sites is classified with the ruggedness index (RIX), provided by the WAsP package, which accounts for the percentage of the surrounding terrain within a radius of 3 km having slopes of more than 30%, a threshold that is typically associated to flow separation. Table II shows the RIX index for the sites in Navarre. A widespread of values from 0 to 29% indicates the large spectrum of site complexities evaluated.

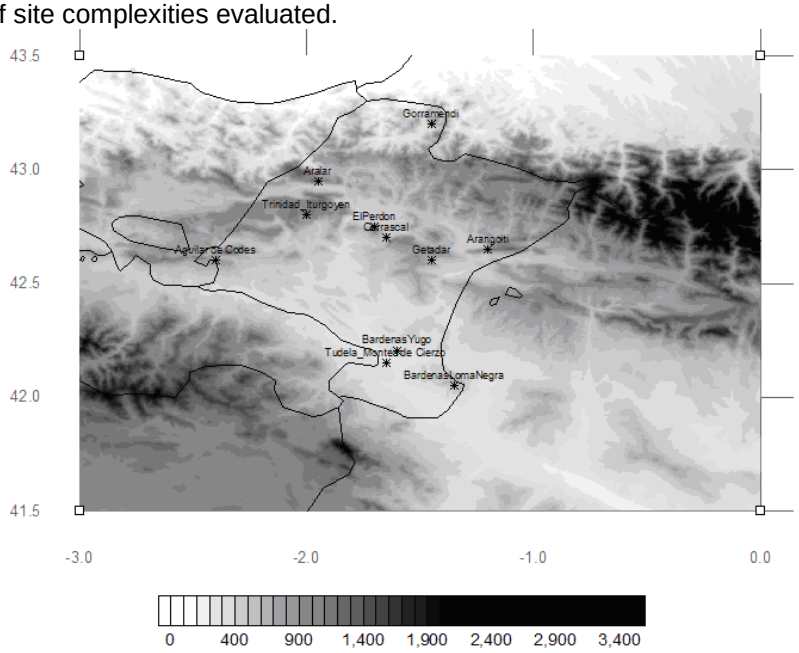

Figure 3. *Sites and locations on the elevation map over Navarre and surroundings. The elevation data are from SRTM. (http://www2.jpl.nasa.gov/srtm/). Coordinates in Latitude/Longitude system.*

Table 2: *Details of measurements for the sites in Navarre.*

Name	Lat-N [º]	Lon-E [º]	RIX	Time length used	VmeanH	VmxH	Vmx10	Weibull Parameters	
	WGS 84				[m/s]			A	k
Aguilar de Codés	42.61	-2.39	8.5	December 2003-November 2010	**4.0**	16.2	18.5	4.3	**1.57**
Aoiz	42.79	-1.37	22.4		2.3	13.8	16.6	2.7	1.84
Aralar	42.95	-1.96	19.0		**6.6**	31.7	33.3	7.8	**2.14**
Arangoiti	42.65	-1.19	26.0		**7.5**	25.8	29.1	9.0	**1.85**
BardenasLomaNegra	42.07	-1.37	3.5		**7.2**	29.3	31.6	8.0	**1.62**
BardenasYugo	42.21	-1.58	0.4		**5.3**	20.7	22.5	6.0	**2.16**
Carcastillo	42.37	-1.46	0.0		2.7	13.0	16.3	3.1	1.59
Carrascal	42.68	-1.66	2.6		**6.4**	22.0	23.5	7.2	**1.97**
Doneztebe	43.13	-1.66	11.2		1.3	8.5	10.3	1.5	1.31
ElPerdón	42.73	-1.71	8.9		**8.0**	32.0	33.1	9.0	**2.04**
Erremendia	42.88	-1.18	4.4		2.2	11.3	13.0	2.5	1.58
Estella	42.68	-2.03	1.5		2.0	11.7	12.1	2.3	1.74
Etxarri	42.91	-2.06	3.9		2.2	16.9	18.7	2.4	1.21
Getadar	42.62	-1.47	6.6		3.0	12.1	13.6	3.4	1.70
Gorramendi	43.21	-1.45	29.0		**7.5**	37.8	42.1	8.5	**1.65**
Oskotz	42.96	-1.76	3.9		1.4	15.5	18.0	1.8	1.61
Tafalla	42.52	-1.68	0.0		2.6	13.5	15.1	3.0	1.56
Trinidad_Iturgoyen	42.81	-1.98	6.8		**7.3**	28.7	29.8	8.2	**2.09**
Tudela_Montes de Cierzo	42.13	-1.65	0.0		**4.0**	16.1	18.2	4.5	**1.75**
Urbasa	42.85	-2.17	6.7		2.0	9.6	10.7	2.4	1.84
Villanueva_Yerri	42.74	-1.95	0.7		1.9	17.6	19.9	1.9	1.07
Yesa	42.62	-1.19	11.8		2.6	12.3	13.1	3.0	1.65

4. Models and data

4.1 Global models and data

The global data that are used directly in this WP include the reanalysis data from NCEP/NCAR and analysis data from NCEP (GFS).

The NCEP/NCAR reanalysis data are available since 1948 but the data quality is best in the period of 1979 - present, the modern satellite era. The spatial horizontal resolution is about 250 km for most variables but is about 200 km for the 10 m winds and pressure field on Gaussian grids. Data are 6 hourly. This data set is used for (i) identifying extreme wind events in the selective dynamical downscaling method (ii) obtaining Vref with the spectral correction method.

The GFS analysis data are available since 1999. The horizontal resolution is about 1°. Data are also 6 hourly. This data are used as boundary forcing for the mesoscale modelling of WRF (at Risoe) and SKIRON (at Cener).

There are several other meteorological databases we used within the project, including ERA-Interim reanalysis, see Section 7.2.2.1.

4.2 Mesoscale models

Several mesoscale models or their simulated data are used in this WP. For some (REMO, HIRHAM5), we only used their outputs. For the WRF model (section 4.2.1) and the SKIRON model (section 4.2.2), we use them to simulate the winds to obtain the wind and extreme wind statistics.

4.2.1 WRF

The WRF Advanced Research WRF (ARW) core was used for the mesoscale modelling for the selective dynamical downscaling method (section 5.1) to obtain the extreme wind atlas. The 1° GFS data are used as the initial and boundary forcing. Compared to the NCEP/NCAR reanalysis data, the spin-up time of using the FNL data for the simulation is much shorter; it is only a few hours instead of half a day. Because of the better horizontal resolution of the GFS data, the storms are already much better described at the beginning. The storms over the two areas, Denmark and Gulf of Suez, normally do not last more than 2 days, therefore the simulation is limited to 2 to 3 days. Together with the FNL data, the half degree sea surface temperature from NCEP is used. This simulation was done by Risoe DTU.

4.2.2 SKIRON NWP

The Regional Weather Forecasting System SKIRON has been developed for operational use at the Hellenic National Meteorological Service (HNMS). Its central component is the Eta limited-area weather forecasting model. The Eta Model is a state-of-the-art atmospheric model used for research and operational purposes.

The Eta model is formulated as a grid-point model. Partial differential equations are represented by finite-difference schemes in the model. Option to run the model in a non-hydrostatic mode is chosen.
In the horizontal, the model is defined over the semi-staggered E grid. The model uses the Eta coordinate – a generalized sigma coordinate system. The mountains in the Eta system are represented as grid-box mountain blocks. The nonslip bottom boundary condition is used at the vertical sides of the model mountains.

A brief description of Cener's methodology with Skiron is given below:

- GFS is used by Skiron as input and boundary conditions, daily downloaded and stored of GFS 12UTC.
- In addition to GFS, daily SST, Snow cover and Snow depth files are downloaded.
- Horizontal resolution: 0.05ºx0.05º (~5kmx5km); Number of vertical levels: 50 Eta levels.; No nesting; Output frequency = 1h (52h horizon) Model time step = 15 sec.

- Domain configuration: depending on the region of interest, the domain will be able to capture the synoptic patterns governing the meteorology.

4.2.3 Other models and data

Outputs from other two regional climate models, REMO and HIRHAM, are used in connection with the development of the spectral correction method as described in Section 5.2.

The regional climate model REMO is a three dimensional hydrostatic atmospheric model, developed from the Europa-Modell of German Weather Service. It uses the standard setup without nudging technique. The initial and boundary conditions are provided by the reanalysis data ERA-15 for the period 1979 – 1993 and by ECMWF analysis data for 1994 – 2003. Both of the large-scale forcing data have the horizontal resolution of 120 km. REMO was first nested with a horizontal resolution of 50 km using one-way nesting technique and again nested with a horizontal resolution of 10 km using a double nesting strategy. The physical parameterization package of ECHAM version 4 is implemented. This simulation was done by Max Planck Institute for Meteorology in Hamburg, Germany. More details about the model can be found in Jacob and Podzun (1997) and Jacob et al. (2007). The simulation thus covers 1979 – 2003.

The HIRHAM5 combines the dynamical core of the numerical weather prediction model HIRLAM version 7 and the physical parameterization schemes of the global climate model ECHAM version 5, ECHAM5. Details are available in e.g. Christensen et al. (2006). The data analyzed here are from two HIRHAM5 runs, with one driven by the global data from ECHAM5 and another driven by reanalysis data ERA-40. The global data are downscaled directly to 25 km resolution without nesting. No spectral nudging is used. There are 19 vertical layers. The simulation covers the period 1961 – 1990 and it is done by the Danish Meteorological Institute.

4.3 Microscale models

4.3.1 WAsP 10.0

The software WAsP 10.0 is developed and maintained by Risoe DTU (www.wasp.dk). WAsP is a PC program for predicting wind climates and power productions from wind turbines and wind farms. The predictions are based on wind data measured at stations in the same region. The program includes a terrain flow model, a roughness change model and a model for sheltering obstacles.

The statistical-dynamical downscaling uses WAsP to correct the deficiencies of the mesoscale model in capturing the local speed-up effects introduced by the site topography which are especially important in complex terrain.

4.3.2 WAsP Engineering

The software WAsP Engineering (WEng) is developed and maintained by Risoe DTU (www.waspengineering.dk, Mann et al. 2000). Under the impact of a background forcing, it uses a linear computational model (LINCOM) to calculate the effects of topography and roughness changes on a scale down to meters in the upwind fetches of a particular turbine site, thus to obtain the site-specific wind parameters for turbine design, including Vref.

The output of the selective dynamical downscaling method is designed to be the background forcing for the microscale model as in WEng.

It is still a very challenging task to couple the mesoscale modelling to microscaling. Our contribution through the current project is providing the background wind forcing from the mesoscale modelling of WRF for WEng, through a post-processing procedure (see details in Section 5.1).

5. The annual maximum method

The first two methods as introduced in Section 6 have been developed in connection with the Annual Maximum Method (AMM). When using AMM to obtain e.g. the 50-year wind, the annual wind maxima from n year data are first selected and sorted in ascending order as U_i^{max} where i=1,…,n. Then we use the Gumbel extreme wind distribution (Gumbel 1958) to fit the set of annual wind maxima to obtain

$$U_T = \alpha^{-1} \ln T + \beta \quad (1)$$

The coefficients α and β are obtained through the probability-weighted moment procedure

$$\alpha = \frac{\ln 2}{2b_1 - \overline{U^{\max}}}, \qquad \beta = \overline{U^{\max}} - \frac{\gamma_E}{\alpha} \quad (2)$$

where $\gamma_E \approx 0.577216$ is the Euler constant, $\overline{U^{\max}}$ is the mean of U_i^{max} and b_1 is calculated as

$$b_1 = \frac{1}{n}\sum_{i=1}^{n} \frac{i-1}{n-1} U_i^{\max} \quad (3)$$

The uncertainty of the fitting of U_T can be calculated from uncertainties on α and β:

$$\sigma(U_T) = \frac{\pi}{\alpha}\sqrt{\frac{1+1.14k_T+1.10k_T^2}{6n}} \quad (4)$$

with

$$k_T = -\left(\ln\ln\left(\frac{T}{T-1}\right) + \gamma_E\right) \quad (5)$$

Details of this method can be found in Abild (1994) and the derivation of the uncertainty can be found in Abild (1994) and Mann et al. (1998). The uncertainty due to the fitting is estimated to be the 95% confidence interval and it is obtained by $1.96\sigma(U_T)$.

6. The three methodologies

6.1 The selective dynamical downscaling method

The selective dynamical downscaling method has been applied here to examine its feasibility for complex terrain (as in the Navara region) in comparison with flat terrain (as in Denmark).

Details of this method and data validation in simple terrain and medium complex terrain in the Gulf of Suez can be found in Larsén et al. (2012b). The word "selective" is referring to the selection of the annual strongest wind cases. There are three main steps in applying this method. The first step is to identify the storms that contribute to the extreme wind climate in a particular area using the NCEP/NCAR reanalysis data (NRA). The second is the mesoscale modelling of these storms. The third step is to apply a post-processing procedure to generalize the mesoscale winds, which are required as input for the microscale modelling.

When identifying the extreme wind storms, we used both the geostrophic wind (G) and the surface 10 m winds (U_{10}) from the NRA data. As mentioned earlier that the NRA data are of approximately 250 km horizontal resolution. The time step is approximately 10 min but the data are restored every 6 hours. For the selected area over Denmark, there are 20 grid points on the Gaussian grids. For the Navara region, there are 9 grid points. For each grid point, the dates of the annual maximum G and U_{10} are identified. These dates at all the grid points are then added together. This gives a total 59 storms for the area of Denmark for the period of 1999 – 2010. For the Navara region, the storms from 2011 were also simulated and there are 58 storms for this region 1999 – 2011.

The period of 1999 – 2010 is chosen because we use the fine resolution analysis data (GFS) from NCEP, rather than the longer record of NRA, to drive the mesoscale model WRF. The GFS data are of the horizontal spacing of 1 degree and they are only available since 1999. The WRF ARW-core version 3.1 was used for the modelling of storms. Because of the relatively large scale characteristics of the storms over Denmark, we set the horizontal resolution as 45 – 15 – 5 km (Figure 4). For the complex terrain, we set the horizontal resolution as 18 – 6 – 2 km (Figure 5). The inner-most domain, domain III, is the area where the extreme wind atlases are made. When all storms are simulated, we have 12 annual wind maxima with corresponding wind direction at each and every mesoscale grid point in the domain III.

The post-processing procedure was aimed at one of the most challenging issues in coupling between models of different scales. Generally, it is not at all immediately clear how the mesoscale modelled winds should be put into a microscale model. The concept of the combination of a background wind and a microscale model as in WEng inspired us to convert the mesoscale winds to this background wind, a procedure called "generalization" in Badger et al. (2010) and Larsén et al. (2012b). Briefly, in the generalization process the speed-up effects due to local orography and roughness changes in the upstream sectors are calculated and they are represented as the coefficients s_o and s_r, respectively. Here we used 12 sectors. The effective roughness length for each sector z_0 is calculated and it is defined as the area-averaged roughness in the upstream fetches. The effective roughness length and generalization factors form a look-up table for each mesoscale model grid point. For each of the storm episodes, the application of the generalization procedure is done through three steps:

(i) Using

$$u_z = \frac{u_{0,z}}{(1+s_o)(1+s_r)} \tag{6}$$

to convert the simulated wind $u_{0,z}$ to a corrected value u_z.

(ii) Using

$$u_* = \frac{k u_z}{\ln(z/z_0)} \tag{7}$$

and the geostrophic drag law is used to obtain the frictional velocity and the geostrophic wind using the effective roughness length and the corrected wind u_z.

$$G = \frac{u_*}{\kappa}\sqrt{\left(\ln\frac{u_*}{fz_0} - A\right)^2 + B^2} \quad (8)$$

where G is the geostrophic wind and f is the Coriolis parameter.

(iii) Using Equation (8) again for a new roughness length $z_{0,r}$ = 0.05 m, to obtain a new frictional velocity over the same G and use (7) again to obtain the standard wind.

Over water, the coupling of the atmosphere and underlying waves are through the Charnock formulation (Charnock 1955): $z_0 = \alpha_{ch}u_*^2/g$, where the Charnock parameter α_{ch} = 0.018 is used. The Charnock formulation was derived for fully developed wind generated waves over deep water. In the coastal areas, it is seldom the case, especially during stormy conditions. We modified the Charnock coefficient to be 0.05 for the post-processing procedure, based on the measurements from Horns Rev (Peña and Gryning, 2008).

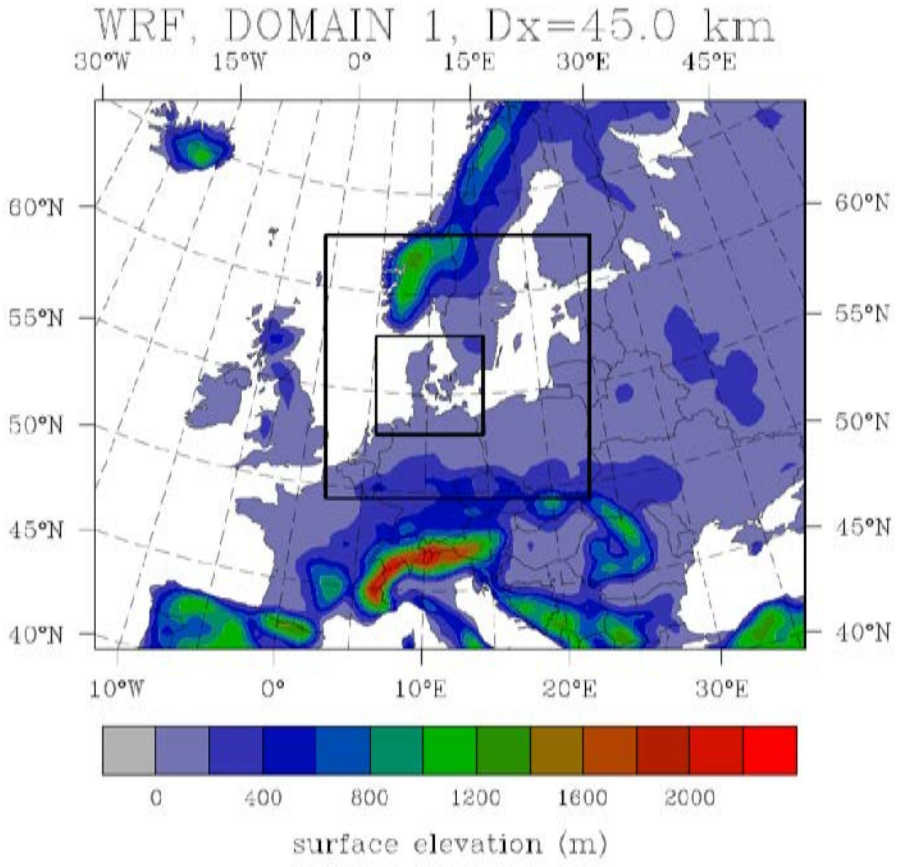

Figure 4. *Three model domains of the WRF modelling over Denmark.*

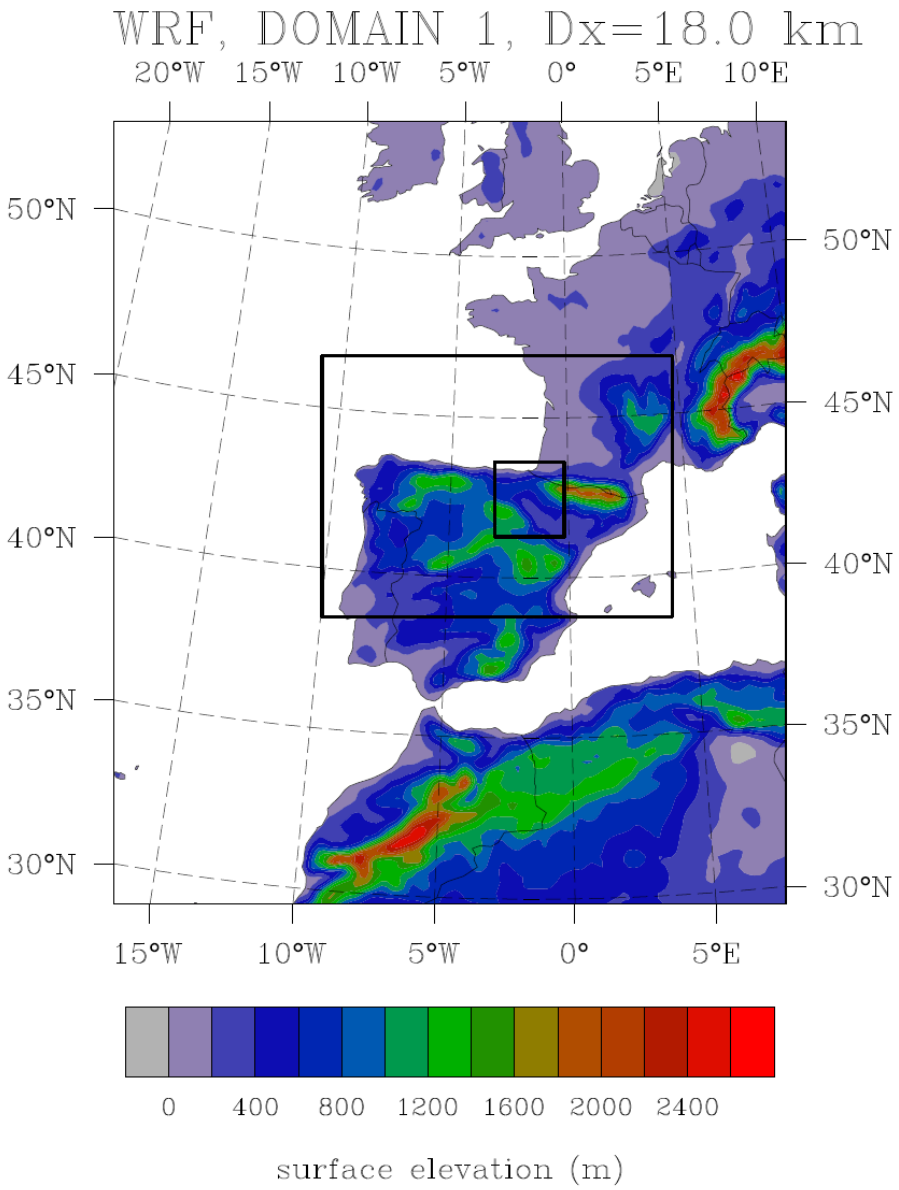

Figure 5. *Three model domains of the WRF modelling over the Navara region in Spain.*

6.2 The spectral correction method

This method can be used to correct the smoothing effect of mesoscale modelling, reflected as the missing variability for the high frequency range, in comparison with measurements (Figure 6). Thus, if the mean wind statistics are well simulated for a site by the mesoscale model, this method can be used to improve the zero and second order moments of the wind speed spectrum from the modelled time series and thus correct the annual wind maximum. Details of this method can be found in Larsén et al. (2012a). It is assumed that the once per year exceedance F follows a Poisson process $F=\exp(-\lambda T_0)$, where T_0 is the period of 1 year and λ is the occurrence rate calculated with

$$\lambda = \int_0^\infty P(u,\dot{u})\,\dot{u}\,d\dot{u} = \frac{\sigma_{\dot{u}}}{\sqrt{2\pi}} P(u) \qquad (9)$$

With $P(u,\dot{u})$ the conditional probability of u, $\dot{u}$ is the time derivative of u, and it is assumed that u and $\dot{u}$ are independent. Here u is the time series of wind speed minus its mean value. Later we use $\bar{u}_{\max}$ as the annual wind maximum from the wind time series minus its mean. With a large threshold, such a distribution of the exceedance is valid for a Gaussian process for which

$$P(u) = \frac{1}{\sigma_u \sqrt{2\pi}} \exp\left(-\frac{u^2}{2\sigma_u^2} \right) \tag{10}$$

Substituting (10) into (9) gives

$$\lambda = \frac{1}{2\pi} \frac{\sigma_{\dot{u}}}{\sigma_u} \exp\left(-\frac{u^2}{2\sigma_u^2} \right) \tag{11}$$

Which is equivalent to

$$\lambda = \frac{1}{2\pi} \sqrt{\frac{m_2}{m_0}} \exp\left(-\frac{u^2}{2m_0} \right) \tag{12}$$

With spectral moments, m_0 and m_2, defined as

$$m_j = 2\int_0^\infty \varphi^2(\omega)\omega^2 S(\omega) d\omega \tag{13}$$

Where S(ω) is the power spectrum of Gaussian process u(t), ω = 2 π f, with φ = $\sin(\omega T_a / 2) / \omega T_a / 2$ a filter due to the temporal resolution, T_a is the averaging time. With this filter, the integration of (13) is done from ω = 0 to ω = 2 π (1/(2T_a)). The integration will converge even when the tails have slopes equal to or greater than -2.

For the maximum wind that occurs once a year, λT_0=1, together with (12) it gives

$$\bar{u}_{\max} = \sqrt{m_0} \sqrt{2\ln\left(\frac{1}{2\pi} \sqrt{\frac{m_2}{m_0}} T_0 \right)} \tag{14}$$

The peak factor k_p is defined as

$$k_p = \frac{\overline{U}_{\max} - \overline{U}}{\sigma} \tag{15a}$$

Thus, the peak factor k_p can be written as

$$k_p = \sqrt{2\ln\left(\frac{1}{2\pi} \sqrt{\frac{m_2}{m_0}} T_0 \right)} \tag{15b}$$

Thus the peak factors and U_{max} with different spectral tails can be estimated. The missing energy in the high frequency range in Figure 6 results in greater difference in the second order moments than the zero order moment and the mean value.

The core of this approach is to replace the spectrum of the modelled winds in the mesoscale range with a spectral slope of -5/3 and extend it to the frequency of 72 day^{-1}, which is the Nyquist frequency of the 10-min time series. The 10-min temporal resolution is chosen in order to be consistence with the standard temporal resolution as suggested by WMO and the IEC standard, which is also used for the selective dynamical downscaling method. As argued in Larsén et al. (2012a) the starting frequency for the spectral correction could be 1 day^{-1}, according to the analysis of the spectrum of the large scale forcing. Or, to be more consistent with the physics, the scale of the integral time scale 1/T could be used. The integral time scale $T=\int_0^\infty \rho(\tau)d\tau$, with ρ the autocorrelation coefficient. T is an average memory time scale representing the geographical weather characteristics (Kristensen et al. 2002, Pope 2000).

The relative underestimation in the dataset of U_{max} should in principle be the same as Vref according to Equations (2) to (4).

In the presence of measurements, be it one year or more, the spectrum used for the correction in the range (1/T, 1/10min) can be obtained from the measurements. In the absence of measurements, the spectral model obtained from Larsén et al. (2012c) is used:

$$S(f) = a_1 f^{-5/3} + a_2 f^{-3} \tag{16}$$

where $a_1 = 3\cdot 10^{-4} m^2 s^{-8/3}$ and $a_2 = 3\cdot 10^{-11} m^2 s^{-8/3}$.

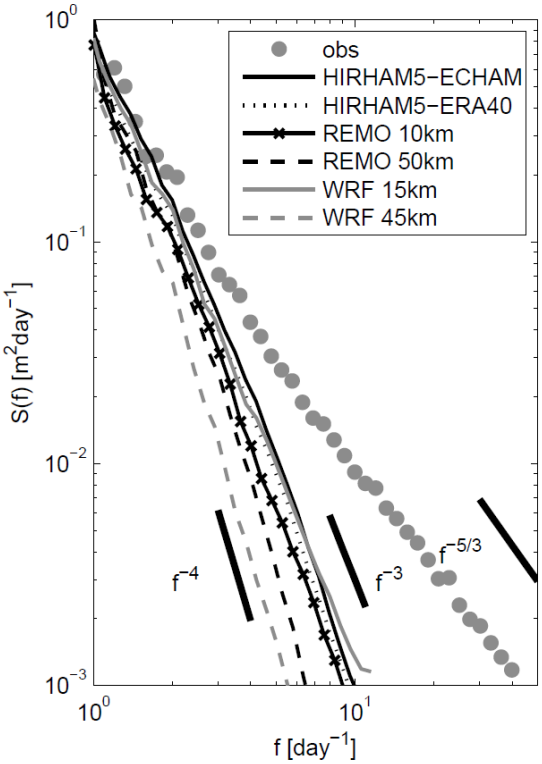

Figure 6: *Spectra of wind speed at 10 m at an offshore site Horns Rev in Denmark, from measurement and six model simulations. Power spectra S(f) versus frequency f. The thick short straight lines show three reference slopes of -5/3, -3 and -4. From Larsén et al. (2012a).*

6.3 The physical-statistical downscaling method using SKIRON

This method is developed to correct the deficiencies of the mesoscale model in capturing the local speed-up effects introduced by the site topography which are especially important in complex terrain. As a result, the 10m NWP velocity is biased towards lower speeds due to a smoother terrain.

With the downscaling method, the high-resolution microscale simulations, with spatial resolutions of some tens of meters, are averaged out to obtain a low-resolution velocity, $U_{10,low}$, which is comparable with the one obtained from the NWP at 10m. The ratio of the high-resolution 10m velocity at mast position, U_{10high}, with respect to the equivalent low-resolution velocity defines the downscaling factor A_d, which can be applied to the NWP 10m wind speed to obtain a corrected time series that includes microscale speed-ups

$$\left[U_{10}(t)\right]_{micro} = \left[U_{10}(t)\right]_{NWP} A_d \tag{17}$$

$$A_d(\theta_{NWP}) = \left[\frac{\overline{U_{10,high}}}{\overline{U_{10,low}}}\left(\overline{\theta_{NWP}}\right)\right]_{micro} \tag{18}$$

In order to take into account the complexity of the terrain, a factor derived from the ruggedness index (RIX value) of the mast location is applied to the results. The ruggedness index has been used to develop an orographic correction factor for WAsP-predictions in complex terrain. The RIX value in percentage, derived from the WAsP program, defines de RIX factor A_{RIX}.

$$A_{RIX} = 1 - RIX\ [\%] \tag{19}$$

$$\left[U_{10}(t)\right]_{micro} = \left[U_{10}(t)\right]_{NWP} A_d A_{RIX} \tag{20}$$

Hence, the RIX factor is introduced in order to attenuate the speed-up correction in complex terrain, where WAsP is likely to produce over-predictions. The RIX correction has been evaluated in the Navarre network resulting in added performance with respect to the RIX-free downscaling method.

7. Results and validation

7.1 From the selective dynamical downscaling method

7.1.1 Flat terrain Denmark

The extreme wind events during 1999 – 2010 that are identified from measurements over Denmark were identified using the NRA data by 100%.

Data are validated in several steps. The time series of wind, direction and pressure are first compared between the point measurement and the values at the closest grid point. The directional distribution of the 10 strongest wind events at each site is examined. The 50-year wind at the measuring height is compared between measurements and simulation and finally, the 50-year standard winds from measurements and simulation are compared. Detailed validation can be found in Larsén et al. (2012b).

Figure 7 shows the maps of the 50-year wind over Denmark and surroundings. The left plot (Figure 7a) is the 50-year wind of the simulated 10 m wind and the right plot (Figure 7b) is the 50-year standard wind. The corresponding values of the 50-year standard wind at a number of stations are listed in Table 3, for both Denmark and Gulf of Suez areas.

Many of our measurement stations are in coastal areas. We have observed greater modelling challenges in the coastal areas, partly because the coupling of atmosphere and ocean waves still needs to be improved and partly because the post-processing is not perfect yet. Overall, the agreement between measurements and simulation is good (Table 3).

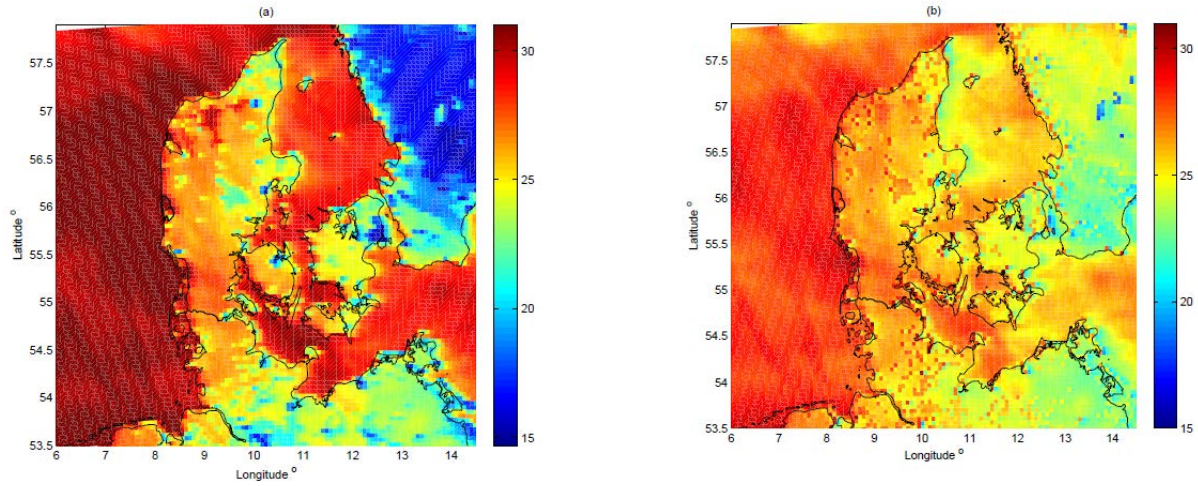

Figure 7: *Map of the 50-year wind over Denmark and surroundings. (a) The 50-year wind at 10 m calculated with 10 m wind speed from the WRF modelling. (b) The 50-year wind of the standard condition through the post-processing procedure. (From Larsén et al. 2012b).*

Table 3*: The 50-year standard wind, i.e. at 10 m, over roughness length of 0.05 m together with 1.96σ from measurement and simulation. Values marked with (*) are from Larsén and Mann (2009).*

	U_{50}, no generalization				$U_{50,st}$, with generalization		
Stations	Height (m)	WRF	OBS	ΔU_{50}	WRF	OBS	$\Delta U_{50,st}$
Sprogø	70	34.2 ± 6.7	33.0 ± 3.7	1.2	24.2±4.4	23.9±2.0 *	0.3
Tystofte	39	31.2 ± 6.6	31.5 ± 4.5	-0.3	25.0±5.4	25.7±2.9 *	-0.7
Kegnæs	23.4	31.2 ± 7.0	35.8 ± 7.0	-4.6	25.8±5.5	26.3±3.8 *	-0.5
Jylex	24	31.8 ± 6.4	35.4 ± 5.5	-3.6	27.4±5.4	29.1±2.9 *	-1.7
Risø	76.6	32.0 ± 6.3	33.2 ± 5.4	-1.2	25.6±5.3	23.7 ± 4.7	1.9
Høvsøre	100	39.5 ± 8.0	44.6 ± 12.5	-5.1	29.7±5.8	29.8 ± 9.4	-0.1
Horns Rev	62	39.3 ± 7.7	44.2 ± 14.0	-4.9	29.0±5.3	31.6±8.5	-2.6
FINO1	50	36.5 ± 6.0	38.1 ± 8.8	-1.6	27.8±4.3	27.4±7.6	0.4

7.1.2 Complex terrain Navara region

The maps of the 50-year wind at 10 m are shown in Figure 8, (a): without post-processing and (b): with post-processing.

The philosophy of data validation in this section is different from that given in Section 6.3 for the physical-statistical downscaling method using SKIRON. While it is questioned about the reliability of the linear model LINCOM for very complex terrains in the post-processing procedure for the selective dynamical downscaling method, we dropped the validation approach as done to the flat terrain Denmark case. RIX, as in Table 3 and Section 6.3, are calculated from WAsP from a rather small area around the site; for many of the low RIX sites, only several kilometres away, there are cliffs and mountains, e.g. Tudela and Loma Negra. In these complex terrains, flow separation occurs and this cannot be taken into account in the linear model which is expected to considerably overestimate the speedup effect. Although, for the mesoscale terrain and roughness, such flow separation issue is expected to be less serious than the microscale site conditions and therefore Figure 8b is produced. In Table 3, the 50-year winds calculated with outputs from WRF for 1999 – 2011 and WRF for 2003 – 2010 (overlapping period with the measurements) are listed. The difference is not very big except for the larger fitting uncertainty related to shorter data sets. The 50-year wind from measurements are also given in Table 3; the numbers in the parentis are 10 min values corrected from 1 hour values using the model for disjunctive sampling rate in Larsén and Mann (2006). While it can be seen that for the relatively flat terrain sites, Yugo and Carrascal, WRF provides reasonably good estimates, for the complex terrains, WRF in general gives deviated values, either overestimating or underestimating.

To show the spatial complexity of terrain and roughness and their impact on the spatial distribution of the 50-year wind, in Figure 9, the 50-year wind at 10 m and 50-year standard winds are plotted for the 11 sites listed in Table 3, over areas with 11 by 11 grid points, corresponding to 20 km by 20 km. The the middle point is the grid point closest to the site (marked by the red dot). It is quite clear that a high horizontal resolution is needed for the model runs. With 5 km distance (the horizontal resolution of Skiron), the winds in the “flattest” site Tudela can vary by 10 m/s already. How to make use of the mesoscale modelled data is a challenging question. For the most difficult site Gorranmendi, the 50-year standard wind from the selective dynamical downscaling method is 30 m/s. In order to predict a local extreme wind of 47 m/s as observed, the speedup effect should be about 50%.

While we have avoided using the procedure as used for the Denmark case, namely to obtain the 50-year standard winds and put it into the microscale model LINCOM, because of the limit of linear model in such a complex terrain, we try to estimate the extreme wind using the results from the selective dynamical downscaling method and the spectral correction method in Section 7.3.2.

Table 3: *The 50-year wind ± 1.96σ without post-processing, from WRF with the entire period 1999 – 2011 (WRF(a)), from WRF with overlapping period with the measurements (WRF(o)), based on 10 min values. The 50-year winds from measurements (OBS) in the parenthesis are corrected from hourly values to 10 min values*.

		U_{50}, no generalization		
Stations	RIX	WRF (a)	WRF (o)	OBS
Yugo	0.4	26.2±6.2	24.6±5.6	24 (25.2)
Carrascal	2.6	25.2±5.4	24.8±5.8	25 (26.3)
Tudela	0.0	25.5±6.2	25.5±7.1	18 (18.9)
Loma Negra	3.5	28.9±6.8	26.4±5.2	32 (33.6)
Getadar	6.6	19.8±3.3	19.3±3.3	15 (15.8)
Iturgoyen	6.8	26.5±5.5	27.0±6.8	28 (29.4)
Codés	8.5	23.8±5.2	22.4±5.2	18 (18.9)
Perdón	8.9	26.5±5.6	25.9±5.9	36 (37.8)
Aralar	19.0	22.4±4.1	23.4±6.0	32.5 (34.1)
Arangoiti	26.0	21.4±3.6	20.0±3.4	27.5 (28.9)
Gorramendi	29.0	26.7±5.1	26.5±6.3	45 (47.3)

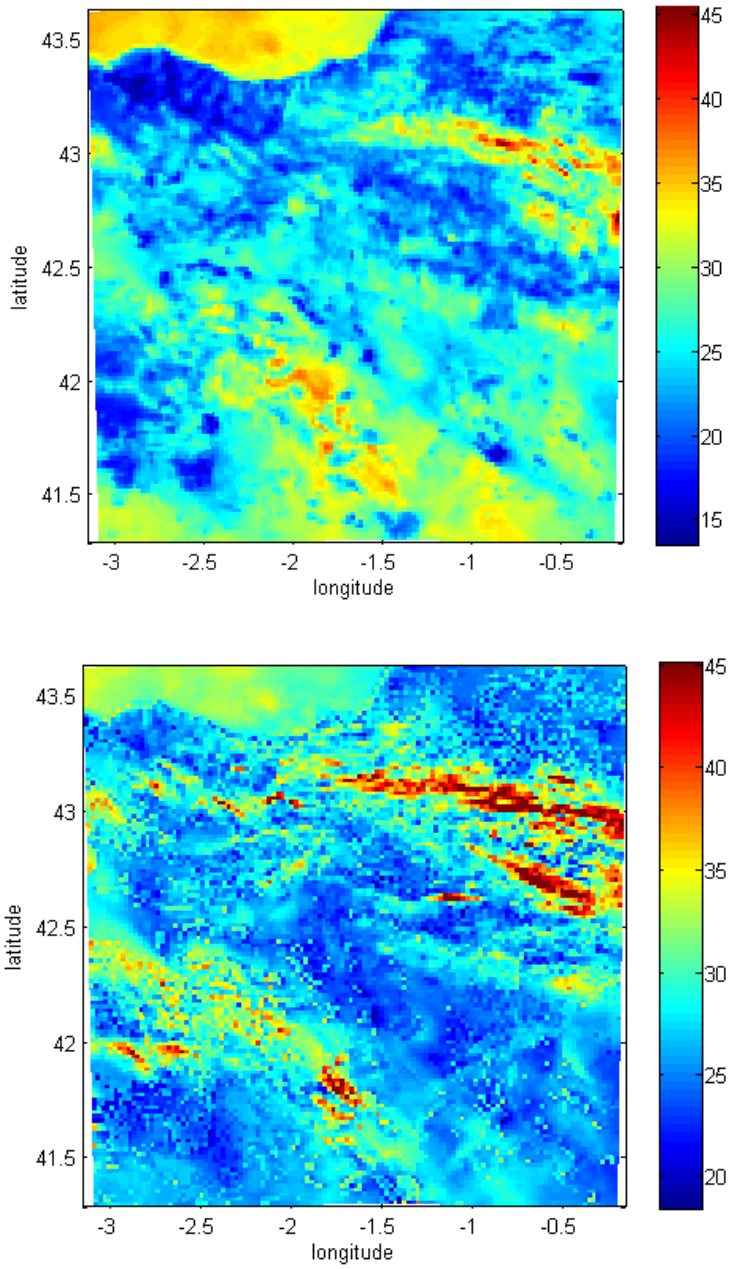

Figure 8: *The 50-year wind at 10 m over the Navara region, (above) without post-processing, (below) with post-processing using the linear model LINCOM.*

Yugo

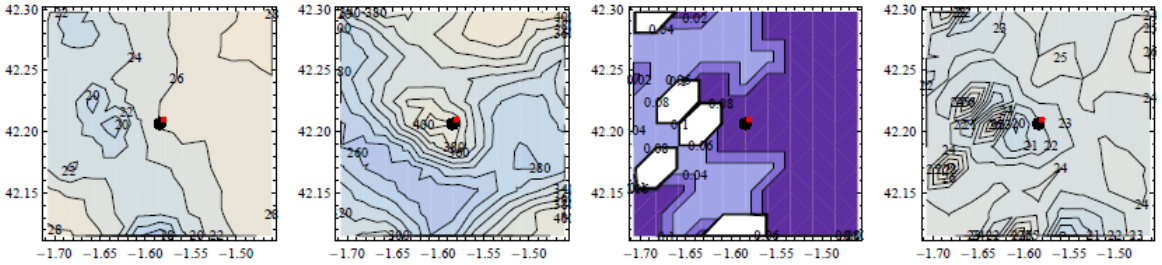

Carrascal

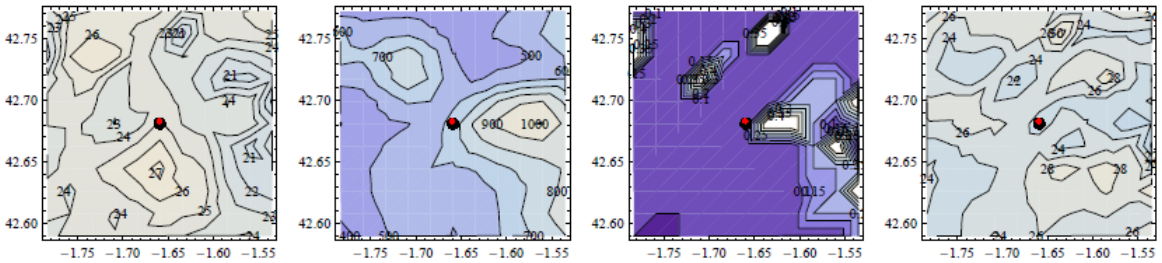

Tudela

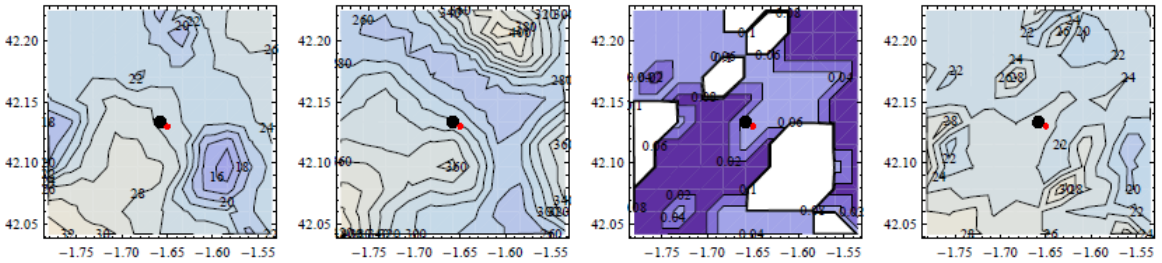

Loma Negra

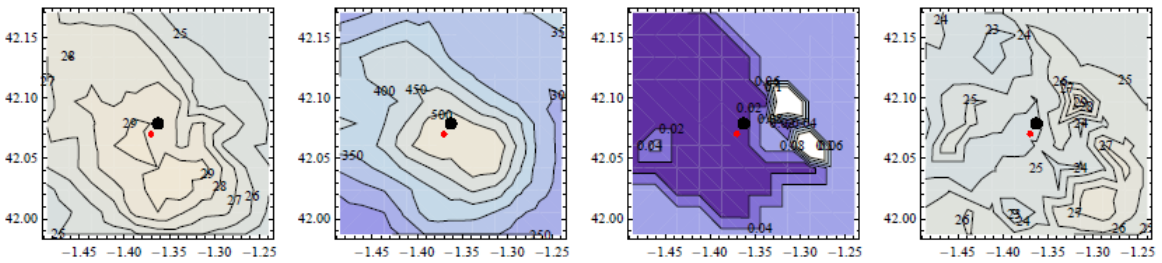

Getadar

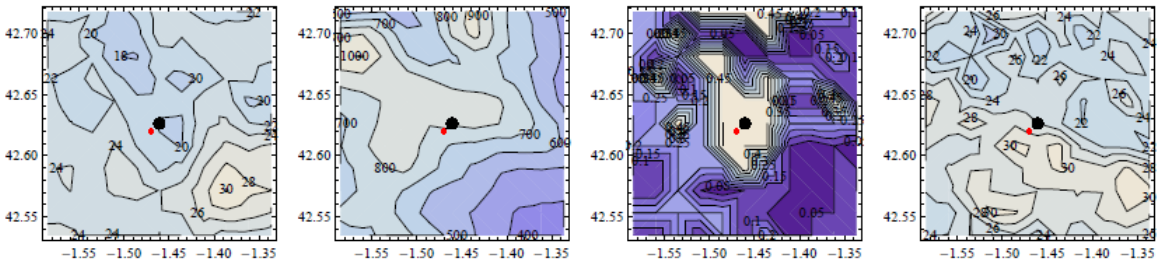

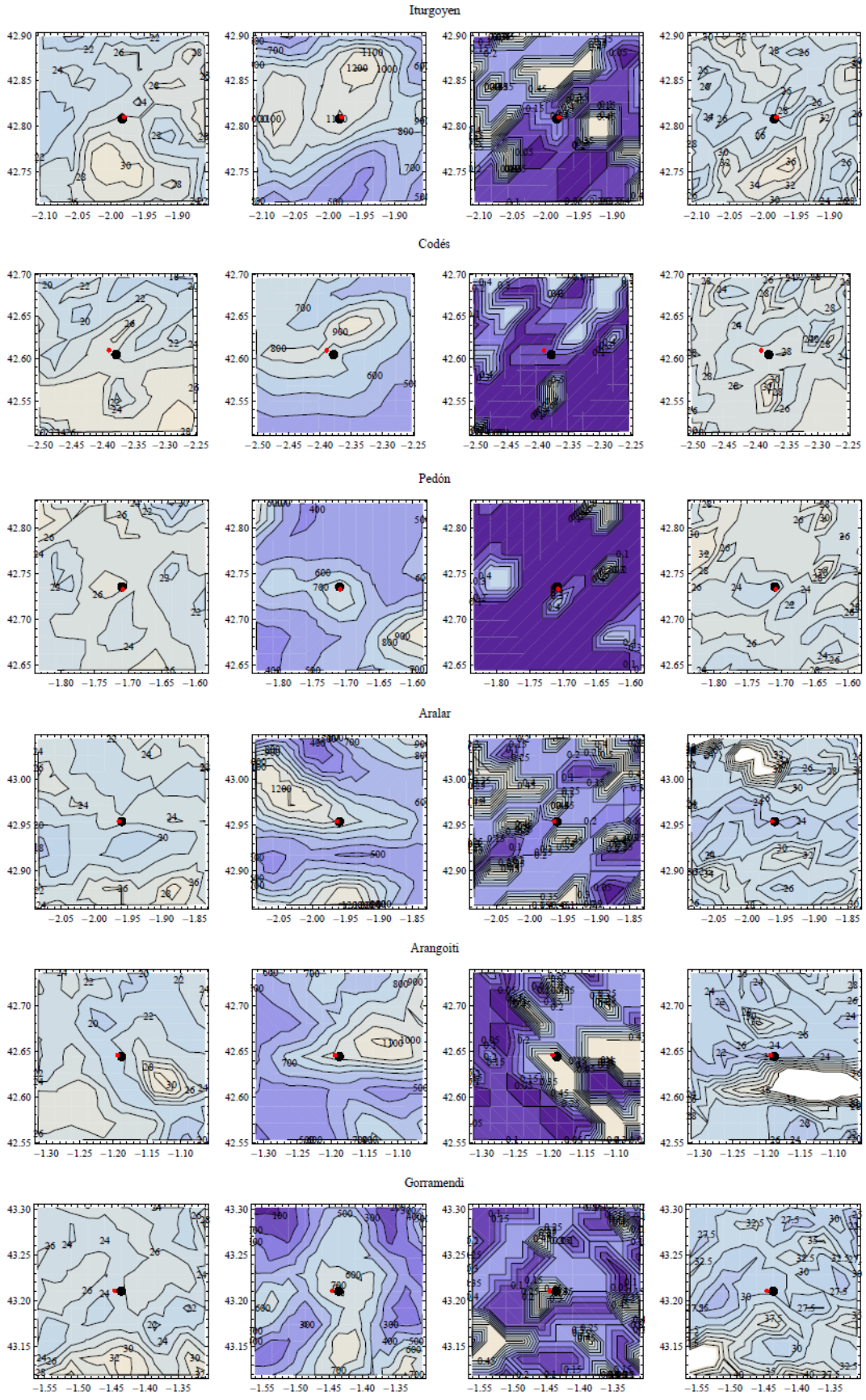

Figure 9: *11 by 11 grid points with the middle one (big black dot) closest to the site (red dot). From left, column 1: 50-year wind at 10 m, column 2: elevation (m), column 3: roughness length (m); column 4: 50-year wind of the standard condition*.

7.2 From the Physical-Statistical downscaling using SKIRON

The aim of the study is to analyze the feasibility of using mesoscale models to estimate Vref according to IEC 61400-1. In order to perform this analysis Vref has been estimated from different resolution data and compared with the Vref estimated from measured data. This method has been applied to the complex terrain Navara region.

Several EVA statistical methods have been compared with the maximum 10 minutes average registered in the seven years period (see Figure 10 for the Navarre test case). The results of this comparison are that:

- IEC method, i.e. Vref=5Vmean, looks like a good rule of thumb but does not account for changes in the wind climate distribution.
- Threshold method tends to underestimate.
- European Wind Turbine Standard (EWTS) method (Winkelaar, 1999) overestimate for k<1.78 and underestimate for k>1.78.
- WEng Gumbel fit, or Annual Maximum Method, has the lowest deviation.

According to these results the statistical method used to estimate Vref with the different resolution data has been the AMM. Hence the EVA method is the same for the three methodologies described in this report.

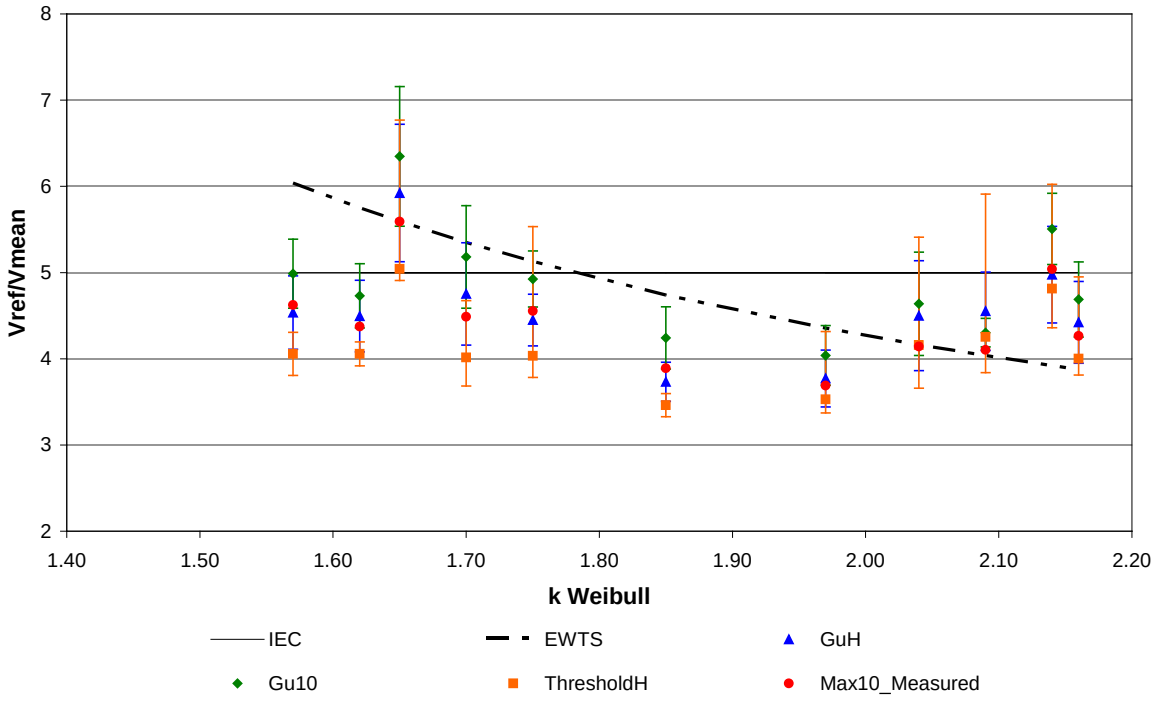

Figure 10: *Comparison between maximum 10 minutes average measured and Vref estimate with several statistical methods for the Navarre test case: Gu10, Gumbel fit with 10 minutes data; GuH, Gumbel fit with hourly data; ThresholdH, threshold method fit with hourly data; Max10_Measured, maximum ten minutes average registered; EWTS, European Wind Turbine Standard fit.*

7.2.1 From the measured data

The wind characteristics in the masts and the Vref estimation for the 10 minutes data and hourly data recorded are presented in Table 4.

Table 4: *At Navarre sites: mean wind speed (Vmean), maximum hourly average (VmxH), maximum 10' average (Vmx10), Weibull parameters (A,k), Vref from hourly data and Vref from 10 minutes data.*

Name	Vmean	VmxH	Vmx10	Weibull Parameters		Hourly	10'
	[m/s]			A	k	Vref	Vref
Aguilar de Codés	4.0	16.2	18.5	4.3	1.57	18.1	19.9
Aralar	6.6	31.7	33.3	7.8	2.14	32.9	36.4
Arangoiti	7.5	25.8	29.1	9.0	1.85	27.9	31.7
BardenasLomaNegra	7.2	29.3	31.6	8.0	1.62	32.5	34.2
BardenasYugo	5.3	20.7	22.5	6.0	2.16	23.3	24.7
Carrascal	6.4	22.0	23.5	7.2	1.97	24.0	25.7
ElPerdón	8.0	32.0	33.1	9.0	2.04	36.0	37.1
Getadar	3.0	12.1	13.6	3.4	1.70	14.4	15.7
Gorramendi	7.5	37.8	42.1	8.5	1.65	44.6	47.8
Trinidad_Iturgoyen	7.3	28.7	29.8	8.2	2.09	33.0	31.2
Tudela_Montes de Cierzo	4.0	16.1	18.2	4.5	1.75	17.8	19.7

Most of the maxima recorded have occurred in days with especial meteorological conditions:

- 27 January 2005, maximum wind in *Bardenas Loma Negra*. Between 23 and 31 of January a cold wave with strong winds affected the north of Spain.
- 25 November 2006, maximum wind in *Arangoiti*. Navarre was in weather alert for high winds.
- 5 and 6 March 2008, maximum wind in *Bardenas Yugo* and *Trinidad iturgoyen.* Navarre was in weather alert for snow and high winds.
- 24 January 2009, maximum wind in *Aguilar de Codés*, *Gorramendi* and *Tudela Montes de Cierzo*. On 24 January 2009 southern France and northern Spain were affected by a severe windstorm associated with extratropical cyclone Klaus.
- 27 February 2010, maximum wind in *Aralar*, *Carrascal* and *El Perdón.* Between end of February and early March, winter storm Xynthia has affected South Western Europe causing storm damage and flash floods along the Breton coast.

7.2.2 From meteorological databases

In order to analyze the feasibility of using meteorological models to estimate Vref according to IEC 61400-1, three different databases have been analyzed for a common period from December 2003 to November 2010:

- ERA-Interim reanalysis, 1.5º spatial resolution and 6 hours temporal resolution.
- GFS, 1º spatial resolution and 3 hours temporal resolution.
- Skiron output for the Iberian peninsula domain (see Figure 11), 0.05º spatial resolution and 1 hour temporal resolution.

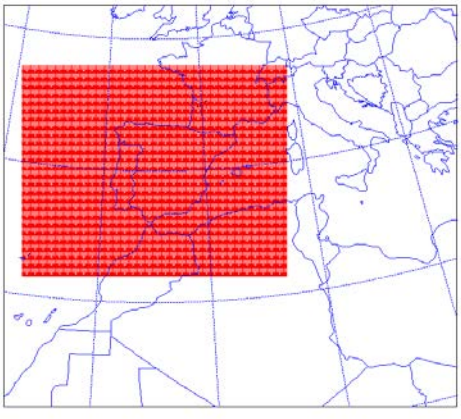

Figure 11: *Domain simulated with mesoscale model Skiron for the Iberian Peninsula*

For the 11 met stations, the nearest grid point has been selected for each of the three datasets (see Figure 12) and mean wind speed, Weibull parameters and Vref estimation has been calculated.

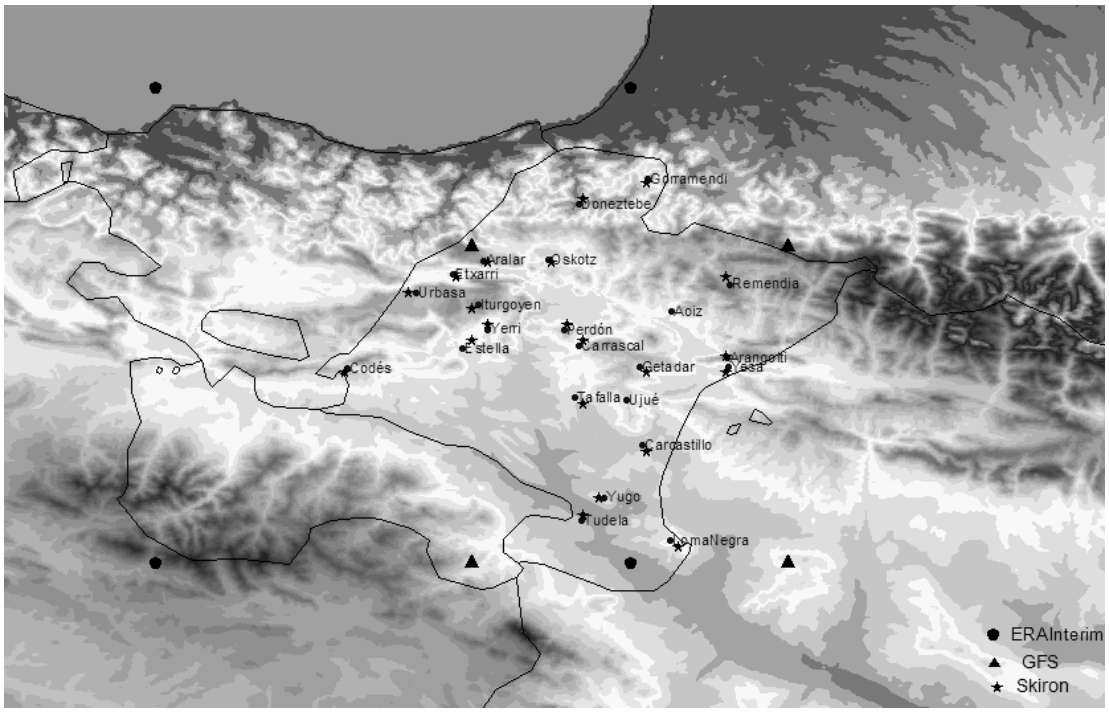

Figure 12: *Navarre met stations and nearest grid points*

7.2.2.1 ERA Interim

The results are presented in Table 5. As expected, the reanalysis data largely underestimate the Weibull k parameter, and the mean and maximum wind speeds.

Table 5: *Mean wind speed, Weibull parameters and Vref estimation for the 11 met masts and ERA Interim nearest grid point.*

Name	Nearest Point	Measured data					ERA Interim				
		Vm	Vmx	k	Vmx/Vm	Vref	Vm	Vmx	k	Vmx/Vm	Vref
Aguilar de Codés	42.0, -3.0	4.0	16.2	1.57	**4.1**	**18.1**	3.3	14.7	1.39	**4.5**	**15.4**
Aralar	43.5, -1.5	6.6	31.7	2.14	**4.8**	**32.9**	2.8	16.5	1.64	**5.8**	**17.2**
Arangoiti	43.5, -1.5	7.5	25.8	1.85	**3.5**	**27.9**	2.8	16.5	1.64	**5.8**	**17.2**
Bardenas Loma Negra	42.0, -1.5	7.2	29.3	1.62	**4.1**	**32.5**	3.1	13.6	1.47	**4.4**	**15.4**
Bardenas Yugo	42.0, -1.5	5.3	20.7	2.16	**3.9**	**23.3**	3.1	13.6	1.47	**4.4**	**15.4**
Carrascal	42.0, -1.5	6.4	22.0	1.97	**3.5**	**24.0**	3.1	13.6	1.47	**4.4**	**15.4**
ElPerdón	42.0, -1.5	8.0	32.0	2.04	**4.0**	**36.0**	3.1	13.6	1.47	**4.4**	**15.4**
Getadar	43.5, -1.5	3.0	12.1	1.70	**4.0**	**14.4**	2.8	16.5	1.64	**5.8**	**17.2**
Gorramendi	43.5, -1.5	7.5	37.8	1.65	**5.0**	**44.6**	2.8	16.5	1.64	**5.8**	**17.2**
Trinidad Iturgoyen	43.5, -1.5	7.3	28.7	2.09	**4.0**	**33.0**	2.8	16.5	1.64	**5.8**	**17.2**
Tudela Montes de Cierzo	42, -1.5	4.0	16.1	1.75	**4.0**	**17.8**	3.1	13.6	1.47	**4.4**	**15.4**

7.2.2.2 GFS

Table 6 presents the results obtained for GFS data. Similar to ERA Interim data, GFS tends to underestimate the Weibull k parameter, and the mean and maximum wind speeds. Nevertheless, the higher resolution of GFS data compared to ERA Interim reanalysis data, introduces corrections that are clearly noticed in complex terrain sites. Note that sites like Tudela, Bardenas-Yugo and Carrascal, characterized by low RIX index, i.e. simple terrain, already produce reasonably good predictions of Vref considering an uncertainty of ±5 m/s that can be generally assumed based on the Gumbel fit error.

Table 6: *Mean wind speed, Weibull parameters and Vref Gumbel estimation for the 11 met masts and GFS nearest grid point*.

Name	Nearest Point	Measured data					GFS				
		Vm	Vmx	k	Vmx/Vm	Vref	Vm	Vmx	k	Vmx/Vm	Vref
Aguilar de Codés	43.0, -2.0	4.0	16.2	1.57	**4.1**	**18.1**	2.1	21.7	1.67	**10.4**	**26.2**
Aralar	43.0, -2.0	6.6	31.7	2.14	**4.8**	**32.9**	2.1	21.7	1.67	**10.4**	**26.2**
Arangoiti	43.0, -1.0	7.5	25.8	1.85	**3.5**	**27.9**	3.0	16.1	1.82	**5.5**	**17.5**
Bardenas Loma Negra	42.0, -1.0	7.2	29.3	1.62	**4.1**	**32.5**	3.3	16.1	1.68	**4.9**	**19.6**
Bardenas Yugo	42.0, -2.0	5.3	20.7	2.16	**3.9**	**23.3**	3.4	17.1	1.87	**5.1**	**19.2**
Carrascal	43.0, -2.0	6.4	22.0	1.97	**3.5**	**24.0**	2.1	21.7	1.67	**10.4**	**26.2**
ElPerdón	43.0, -2.0	8.0	32.0	2.04	**4.0**	**36.0**	2.1	21.7	1.67	**10.4**	**26.2**
Getadar	43.0, -1.0	3.0	12.1	1.70	**4.0**	**14.4**	3.0	16.1	1.82	**5.5**	**17.5**
Gorramendi	43.0, -1.0	7.5	37.8	1.65	**5.0**	**44.6**	3.0	16.1	1.82	**5.5**	**17.5**
Trinidad Iturgoyen	43.0, -2.0	7.3	28.7	2.09	**4.0**	**33.0**	2.1	21.7	1.67	**10.4**	**26.2**
Tudela Montes de Cierzo	42.0, -2.0	4.0	16.1	1.75	**4.0**	**17.8**	3.4	17.1	1.87	**5.1**	**19.2**

7.2.2.3 Skiron

The results are presented in Table 7. The Skiron data tends to underestimate the Weibull k parameter, mean wind speed (Figure 13) in the North of Navarre by more than 2 m/s, and maximum wind speed (Figure 14) in most places by more than 5 m/s. These very large underpredictions are to be expected since they correspond to sites with very complex terrain.

Table 7: *Mean wind speed, Weibull parameters and Vref Gumbel estimation for the 11 met masts and Skiron nearest grid point*.

Name	Near Point	Measured data					Skiron				
		Vm	Vmx	k	Vmx/Vm	Vref	Vm	Vmx	k	Vmx/Vm	Vref
Aguilar de Codés	42.60, 2.40	4.0	16.2	1.57	**4.1**	**18.1**	3.9	19.5	1.57	**4.9**	**20.4**
Aralar	42.95, 1.95	6.6	31.7	2.14	**4.8**	**32.9**	4.9	23.7	1.83	**4.8**	**25.5**
Arangoiti	42.65, 1.20	7.5	25.8	1.85	**3.5**	**27.9**	5.4	23.1	1.62	**4.3**	**25.4**
Bardenas Loma Negra	42.05, 1.35	7.2	29.3	1.62	**4.1**	**32.5**	5.4	20.1	1.61	**3.7**	**22.3**
Bardenas Yugo	42.20, 1.60	5.3	20.7	2.16	**3.9**	**23.3**	3.7	16.0	1.58	**4.3**	**16.8**
Carrascal	42.70, 1.65	6.4	22.0	1.97	**3.5**	**24.0**	3.8	15.8	1.63	**4.2**	**17.0**
ElPerdón	42.75, 1.70	8.0	32.0	2.04	**4.0**	**36.0**	3.0	15.1	1.58	**5.0**	**17.5**
Getadar	42.60, 1.45	3.0	12.1	1.70	**4.0**	**14.4**	3.6	14.4	1.70	**4.0**	**15.9**
Gorramendi	43.20, 1.45	7.5	37.8	1.65	**5.0**	**44.6**	3.8	21.0	1.39	**5.5**	**24.3**
Trinidad Iturgoyen	42.80, 2.00	7.3	28.7	2.09	**4.0**	**33.0**	4.5	17.9	2.01	**3.9**	**20.7**
Tudela Montes de Cierzo	42.15 ,1.65	4.0	16.1	1.75	**4.0**	**17.8**	3.5	15.8	1.68	**4.5**	**16.6**

7.2.3 Downscaling to microscale

A statistical-dynamical downscaling has been applied to Skiron outputs in order to resolve local speed-ups generated by topography. The results are presented in Table 8: downscaling improves mean wind speed (Figure 13) and the maximum wind speed (Figure 14) substantially in sites with complex topography. One site, Arangoiti, overshoots the predictions.

Regarding the assessment of Vref for wind turbine classification based on the IEC 61400-1 standard (Figure 15), Skiron provides a rather homogeneous value for Vref which would imply that all the sites are class III. On the other hand, the downscaling correction provides a more distinct distribution of the IEC class that takes into account the local site characteristics. Mind that the results are based on hourly values in order to have comparable results among the models.

The corrections introduced by downscaling follow in general a good trend and, in all the sites by one (Arangoiti), downscaling corrections follow a good prediction of the wind turbine class (as predicted by the measurements). The reason for the large overprediction of Arangoiti is that the site is sheltered in very complex terrain. That is why the Skiron predictions produce an apparent good match while the downscaling method substantially overcorrects the speed-up factors. In the contrary, a well exposed site like Gorramendi, with a similar RIX index as Arangoiti, produces downscaling corrections that go in the right direction and follow a good assessment of the IEC class.

Based on this preliminary study, it can be concluded that the downscaling method works reasonably well in sites that are well exposed to the prevailing winds, which are the typical conditions for wind turbine sites. Nevertheless, it is necessary to extend the evaluation to a larger number of sites in order to extract more statistically meaningful conclusions.

Table 8: *Mean wind speed, Weibull parameters and Vref Gumbel estimation for the 11 met masts and Skiron downscaling*.

Name	Measured data					Downscaling				
	Vm	Vmx	**k**	**Vmx/Vm**	**Vref**	Vm	Vmx	**k**	**Vmx/Vm**	**Vref**
Aguilar de Codés	4.0	16.2	1.57	**4.1**	**18.1**	3.3	**15.4**	1.63	4.7	**16.2**
Aralar	6.6	31.7	2.14	**4.8**	**32.9**	8.0	**34.8**	1.81	4.4	**38.6**
Arangoiti	7.5	25.8	1.85	**3.5**	**27.9**	11.3	**59.7**	1.18	5.3	**64.9**
Bardenas Loma Negra	7.2	29.3	1.62	**4.1**	**32.5**	7.2	**28.0**	1.62	3.9	**31.7**
Bardenas Yugo	5.3	20.7	2.16	**3.9**	**23.3**	4.5	**20.8**	1.70	4.6	**21.9**
Carrascal	6.4	22.0	1.97	**3.5**	**24.0**	3.9	**17.2**	1.76	4.4	**18.0**
ElPerdón	8.0	32.0	2.04	**4.0**	**36.0**	6.2	**32.1**	1.47	5.2	**38.4**
Getadar	3.0	12.1	1.70	**4.0**	**14.4**	5.9	**21.6**	1.86	3.6	**24.8**
Gorramendi	7.5	37.8	1.65	**5.0**	**44.6**	7.0	**45.0**	1.35	6.4	**50.6**
Trinidad Iturgoyen	7.3	28.7	2.09	**4.0**	**33.0**	6.2	**21.9**	2.13	3.6	**25.2**
Tudela Montes de Cierzo	4.0	16.1	1.75	**4.0**	**17.8**	3.5	**14.5**	1.68	4.1	**15.6**

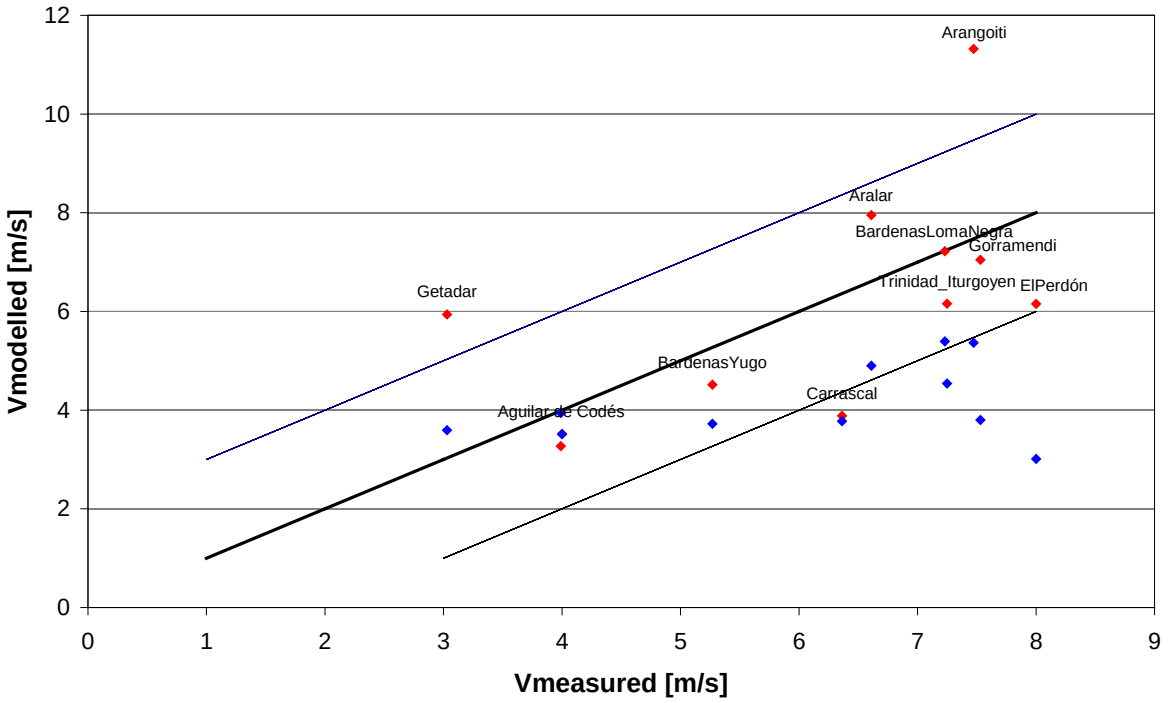

Figure 13: *Mean wind speed for Skiron data (blue squares) and downscaling data (red squares).*

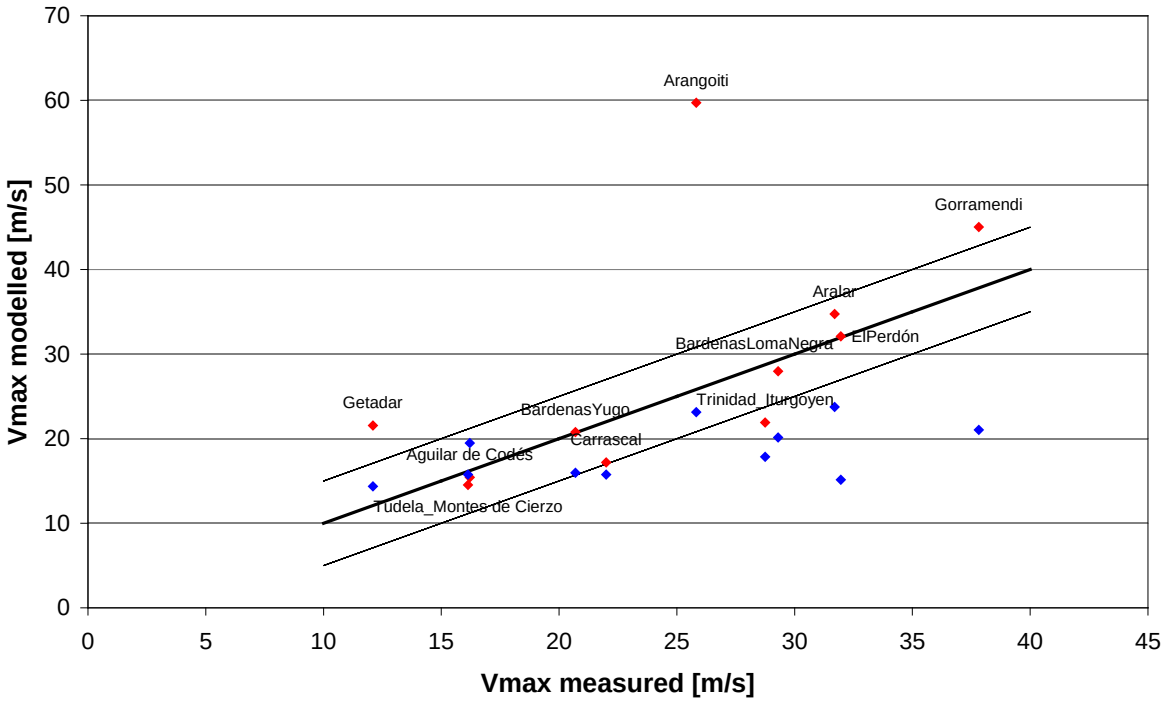

Figure 14: *Maximum hourly wind speed for Skiron data (blue squares) and downscaling data (red squares).*

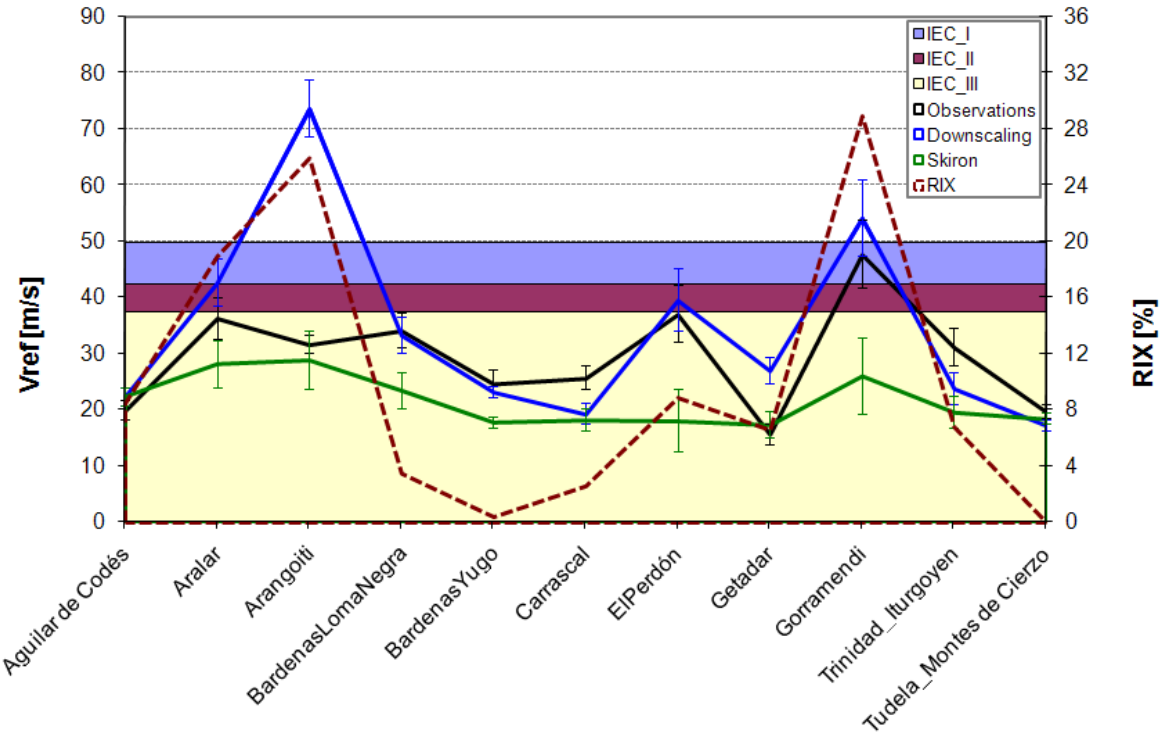

Figure 15: *Gumbel Vref estimation for hourly measured data, Skiron data and downscaling*.

7.2.4 Amplification Factor

The IEC 61400-1 Vref definition is referred to the 10min average instead of the hourly average that characterizes the mesoscale model outputs. Hence, an amplification factor shall be used to estimate the extreme 10-min average wind speed. In order to obtain this amplification factor we have analysed the relation between the maximum 10 min and hourly means, and between the 10 min and hourly Vref in the 11 met masts in Navarre (Table 9).

Table 9: *Relation between 10 minutes maximum and hourly maximum.*

Name	VH_mx	V10_mx	V10_mx/VH_mx	Vref10	VrefH	Vref10/VrefH
Aguilar de Codés	16.21	18.45	1.09	19.90	18.10	1.10
Aralar	31.70	33.32	1.05	36.40	32.90	1.11
Arangoiti	25.82	29.08	1.06	31.70	27.90	1.14
BardenasLomaNegra	29.30	31.63	1.05	34.20	32.50	1.05
BardenasYugo	20.70	22.48	1.09	24.70	23.30	1.06
Carrascal	22.00	23.48	1.06	25.70	24.00	1.08
ElPerdón	31.97	33.14	1.02	37.10	36.00	1.03
Getadar	12.10	13.60	1.12	15.70	14.40	1.09
Gorramendi	37.82	42.11	1.11	47.80	44.60	1.08
Trinidad_Iturgoyen	28.75	29.75	1.03	31.20	33.00	0.94
Tudela_Montes de Cierzo	16.13	18.22	1.06	19.70	17.80	1.11

Considering maximum means the amplification factor from hourly to 10 min is in the range: $1.02 \leq V10/VH \leq 1.12$. Considering Vref, the amplification factor is in the range: $1.03 \leq Vref10/VrefH \leq 1.14$. There is one station showing a Vref amplification factor below 1, which shall not be considered due to large errors in the Gumbel fit. Since both ranges are essentially the same, as a rule of thumb, the maximum hourly mean or Vref velocity can be amplified by 5% to produce a 10min estimate.

Using the site-specific amplification factors we can scale the hourly Vref values presented in Figure 15 to 10 min values. All the sites remain in the same class that was obtained from hourly data.

7.3 From the spectral correction method

7.3.1 Simple terrain

The spectral correction method has been used to calculate the peak factors at the model grid points closest to measurement stations, which are compared to the results from measurements. The offshore site Horns Rev is chosen to be the test case because of the relatively simple surface conditions that are quite consistent in different models.

At the offshore site Horns Rev the measurements give k_p = 4.97. The corresponding peak factors from the hourly time series of the six simulation outputs varies between 4.07 to 4.18, which are significantly smaller than that from the measurements. Using the spectral correction these values are corrected to be between 4.91 and 4.97, which could be considered to be in good agreement with the measured value.

Table 10. *At Horns Rev, mean annual wind speed ($\overline{U}$) and standard deviation (σ), mean annual wind maximum ($\overline{U}_{\max}$) and the standard deviation of the maxima $\sigma_{U_{\max}}$ directly from the time series, measurements (10 min) and modelling (1h), all at 10 m. The integral time scales T are listed too.*

variables	OBS	HIRHAM5		REMO		WRF	
		ECHAM5	ERA40	10 km	50 km	15 km	45 km
$\overline{U}$ (ms^{-1})	7.69	8.22	7.77	8.13	7.95	8.21	7.81
σ (ms^{-1})	3.61	3.72	3.58	3.74	3.77	3.72	3.61
$\overline{U}_{max}$ (ms^{-1})	**27.2**						
$\sigma_{U_{max}}$ (ms^{-1})	5.1						
$\overline{U}_{max,1h}$ (ms^{-1})		23.5	23.8	22.5	23.1	23.2	21.6
$\sigma_{U_{max,1h}}$ (ms^{-1})		2.0	2.3	2.0	1.8	2.4	1.6
T (day)	0.82	0.77	0.83	1.02	0.96	0.83	1.02

Table 11. *At Horns Rev, peak factors from the hourly simulated time series and the corrected values ($k_{p,1h}$ and $k_{p,corr}$) and corrected annual wind maximum using* $\overline{U}_{\max,corr} = \overline{U} + k_{p,corr} \cdot \sigma_{corr}$ *and* $\overline{U}_{\max,corr} = \overline{U}_{\max,1h} \cdot \frac{\overline{U} + k_{p,1h}\sigma}{\overline{U} + k_{p,corr}\sigma_{corr}}$.

Variables	HIRHAM5		REMO		WRF	
	ECHAM5	ERA40	10km	50km	15km	45km*
$k_{p,1h}$	4.18	4.17	4.13	4.10	4.17	4.07
$k_{p,corr}$	4.95	4.94	4.91	4.91	4.94	4.97
$\overline{U}_{\max,corr}$ (m/s)	27.0	25.8	26.7	26.8	26.9	26.7
$\overline{U}_{\max,corr,ts}$ (m/s)	26.3	26.7	25.3	26.1	26.0	24.7

The corresponding values of the annual wind maxima from the hourly simulated time series, ranging from 21.6 to 23.5 m/s (Table 10) are corrected to be between 25.8 to 27.0 m/s by using $\overline{U}_{\max,corr} = \overline{U} + k_{p,corr} \cdot \sigma_{corr}$, with both $k_{p,corr}$ and σ_{corr} the corrected values, or corrected to be between 24.7 to 26.7 m/s using $\overline{U}_{\max,corr} = \overline{U}_{\max,1h} \cdot \frac{\overline{U} + k_{p,1h}\sigma}{\overline{U} + k_{p,corr}\sigma_{corr}}$ (Table 11).

7.3.2 Complex terrain

That the wind variability is much more significant in complex terrain compared to flat terrain has been observed by e.g. Stathopoulos et al. (2012). This is demonstrated here in Figure 16 where the power spectra of wind speed from Carrascal and Gorramendi are plotted together with the spectrum from an offshore site Horns Rev from Denmark. Even though Carascal is a site with rather low RIX, it is not a simple terrain site in mesoscale sense (Figure 9). The wind power spectrum contains less variability than the more complex terrain Gorramendi but significantly more than the flat site Horns Rev. The energy deviation starts somewhere 1.8 10^{-4} Hz, corresponding to 1.5 hours. The mean wind speed at this site is about 6 m/s. Thus the scale where the energy deviation starts is about 30 km around the site. Looking at Figure 9, for the site Carrascal, already in the range of 20 km, there is significant terrain variation between about 500 to 1000m.

The mesoscale modelled storms capture reasonably well the wind variability for the site Carrasca, suggesting most of the variability is on the level of meso scales (Figure 17a). However, the storms modelled for the very complex site Gorramendi miss considerable variability (Figure 17b), suggesting that large part of the variability is related to the local effect. With the mean wind speed about 8 m/s at Gorranmendi, the energy deficit starts at a scale about 60 km around the site.

The above spectral analysis seems to suggest that the complexity of the terrain for the sites needs to take a rather long distance of tens of kilometres around the site into consideration.

The power spectra from the measurements at Corrascal and Gorramenti have been used to correct the extreme wind of the standard condition calculated from the geostrophic winds using NCEP/NCAR reanalysis data. The reanalysis data are of 200 km horizontal resolution on 6 hours basis. The corrected smoothing effects are 38% at Corrascal and 42% at Gorramenti. The value becomes 28 m/s at Corrascal, which is larger than the result from the selective dynamical downscaling method 24 m/s (Figure 9, 2nd row, 4th Column). The 50-year standard wind is 30 m/s at Gorramenti, almost the same as the result from the dynamical downscaling method (Figure 9, last row, 4th Column). At least, the post-processing in the selective dynamical downscaling method provides a good platform here to make comparison with the results from the NCEP/NCAR reanalysis data.

Using the spectral correction approach to correct the WRF modelled variability up to 10 min resolution, the smoothing effect of WRF is only 2% at Corrascal and 5.5% at Gorranmendi (corresponding to Figure 17a and b). The 50-year wind at the grid point closest to the site is corrected to 25.6 m/s from 25.2 m/s at Corrascal, it is corrected to 28.0 m/s from 26.7 m/s (cf. Table 4). Seemingly, for Gorramendi, it is not the mesoscale fluctuation that is missed in the WRF simulated winds; the representativity of the resolution (here 2 km) could be a more related issue. It is not clear if the hourly measurements are sampled at 1 second or 3 seconds and stored on hourly basis or if they are hourly averages. It is difficult to say how well the simulated results are because when comparing with the point measurements from a very unique place such as behind a cliff, the surface condition of the measurements is very different from that over 2 km by 2 km area as in the WRF output. According to Table 4, whereas for most sites, even though the 50-year winds from measurements do not always match those from the WRF simulation, they are not completely different taking the fitting uncertainty into account. However, it is not the case with Gorramenti and Aralar; even though, the fitting uncertainty at Gorramenti is 11 m/s and it is 7 m/s at Aralar, the modelled values are still significantly smaller than those from the point measurements. Likely the 2 km horizontal resolution is still too coarse for sites like Gorramenti and Aralar. Further downscaling seems to be needed. For this, in Section 6.3, RIX is used to add the local speedup effect empirically to the Skiron modelled winds. In Section 6.2, in connection with the selective dynamical downscaling method, we have avoided using LINCOM or the model in WAsP to handle the measurements because of the high uncertainty of linear models in complex terrain. The speedup effect according to the WAsP-files provided by CENER is more than 200% at Gorramenti in some sectors, which is very unusual.

So far, with the selective dynamical downscaling method, we do not have a good solution on how to go further from the mesoscale modelled extreme winds to the very complex terrains like Gorramenti. More studies should be done to understand the flow around the mast in Gorramenti. With high frequency

measurements that will be made available, this spectral analysis can be of use and possibly adds values to the current estimation.

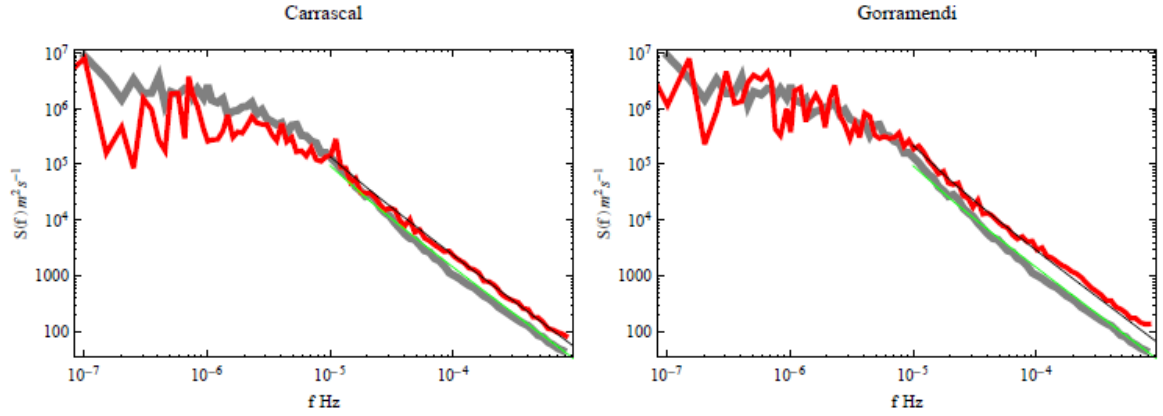

Figure 16. Spectra of the 10 m winds from Carrascal and Gorramendi. The red curves are from measurements. The thick gray curves are from the measurements at the offshore site from Denmark Horns Rev. The green and thin black curves are expression (16), with different coefficients *a*1 and *a*2 for the two terrains.

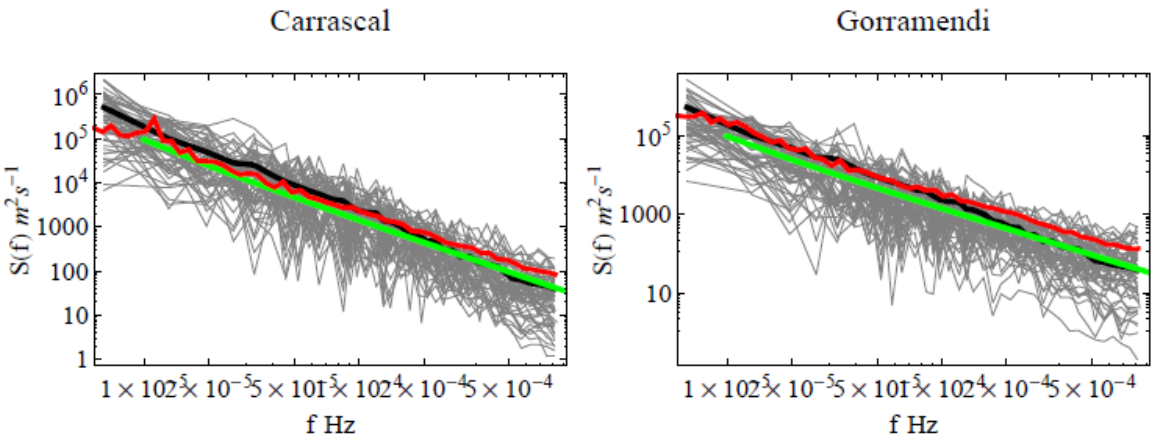

Figure 17. *Spectra of the 10 m winds from each WRF modelled storm time series at the grid point closest to Carrascal and Gorramendi in 62 thin gray lines (62 storms). The average value of the 62 curves is plotted as the thick black curve. The red curve is the same as in Figure 16, from 1-year 10-min measured time series. The green curve is the expression (16).*

8. Discussion, Outlook

Vref assessment will always be compromised by the lack of good quality observational data of sufficient coverage to guarantee good spatial and temporal representativity. Once this fact is acknowledged by the wind energy community, the only practical solution remains the adoption of a standard that can be mutually recognized as a robust and safe approach to the determination of this design parameter.

The use of meteorological models is a very attractive approach since it can avoid many of the shortcomings of the historical observatories, notably: the long-term homogeneity inherent in the philosophy of global reanalysis databases and the trans-national consistency of the method. The continuous improvement of the reanalysis products, both in terms of the quantity and quality of the assimilated observations and in terms of the spatial resolution of the models, encourages the development of methods that use these databases as input data. Then, physical downscaling down to microscale level seems to be the best way of producing wind conditions assessment without the need

of onsite measurements. This area of research is nowadays one of the top priorities for both the wind engineering and meteorology communities.

Physical downscaling methodologies contribute to the development of wind mapping techniques that are being very useful spatial planning instruments. The possibility of predicting the design wind speed besides the expected energy production at microscale level will be a very powerful tool for early site assessment studies. Nevertheless, an accurate assessment will always require the use of onsite measurements, but this kind of tools will help improving the selection of suitable sites and will shorten the measurement campaigns.

Since onsite measurements are sooner or later available at the site, the development of statistical downscaling methods is also important. These techniques make use of site measurements to characterize the high-frequency end of the spectrum, precisely there where mesoscale models are limited. A clever combination of numerical simulations and statistical (spectral) methods seem to offer the most efficient solution for Vref assessment when site measurements are available.

9. Conclusions

Risø's selective dynamical downscaling methodology has shown to be quite accurate in estimating the extreme winds in simple terrains in Denmark and medium complex terrains in the Navara region. The crux is how to apply this method in very complex terrains where we have hesitations to put the extreme winds of the standard condition to the linear model LINCOM for site use.

Risø's spectral correction method can be of general use for mesoscale modelled winds. For simple terrains such as in Denmark, or medium complex terrains in the Navara region, the spectral behaviour is simple and the horizontal resolution of the mesoscale model does not have to be very fine. In very complex terrain such as Gorramendi, the temporal and spatial resolution issue becomes very critical. High resolution dynamical modelling together with high frequency measurements is expected to improve the extreme wind estimation in such places.

CENER's physical-statistical downscaling methodology for the generation of high-resolution virtual time series has been applied to the assessment of extreme winds. This technique is particularly useful in complex terrain where speed-up factors generated by local topography dominate the microscale flow. The technique has proved useful in correcting the large bias of mesoscale models at predicting the mean wind speed in complex terrain sites. It has been shown that the bias is also significantly reduced for the annual maxima and, therefore, reasonably good results are obtained in the assessment of Vref and IEC classification. Out of the 11 sites of the complex terrain test case, only one missed the right IEC class due to the particularly high sheltered conditions of the site. In well exposed sites, typical of wind energy, the results seem to give a consistent result which encourages the development of this technique. Nevertheless, the validation is still limited to a few sites and it is necessary to extend the study to other wind climate and site conditions in order to be able to give more statistically meaningful conclusions.

The presented methodologies constitute clear alternatives for Vref assessment in the initial stages of the planning phase of wind energy, when onsite measurements are of limited duration. As the historical records on the site extend for several years, there shall be a transition to statistical techniques that progressively put more weight on the observations. How this transition is made is something to be developed in the future.

10. Acknowledgement

The NCEP/NCAR data are provided by the NOAA-CIRES Climate Diagnostics Centre, Boulder, Colorado, from their website at http://www.cdc.noaa.giv/. The FNL data are from the Research Data Archive, which is maintained by the Computational and Information system Lab at NCAR. We acknowledge DONG Energy for the measurements from Horns Rev and EU Norsewind project for the measurements at FINO1.

11. References

Abild J. Application of the wind atlas method to extremes of wind climatology. *Technical Report Risoe-R-722(EN)*, Risø National Laboratory, Roskilde, Denmark 1994.

Astrup P, Jensen NO, Mikkelsen T. Surface roughness model for LINCOM. *Technical Report Technical Report R-900*, Risø National Laboratory, Roskilde, Denmark, *URL:www.risoe.dk* 1996.

Badger J, Larsén XG, Mortensen N, Hahmann A, Hensen J, Jørgensen H. A universal mesoscale to microscale modelling interface tool. European Wind Energy Conference, Warsaw, Poland, 20 - 23 April, 6 pages, 2010.

Charnock H. Wind stress on a water surface. *Q. J. R. Meteorol. Soc.* 1955; **81**:639–640.

Clausen N.E. et al. 2009: Are we facing increasing extreme winds in the future? EWEC 2009, conference proceedings.

Dee DP, et al. (2011) The ERA-Interim reanalysis: configuration and performance of the data assimilation system, *Quart. J. R. Meteorol. Soc*., **137**: 553-597

Eurocode. Eurocode 1, Basis of design and actions on structure – Parts 2 – 4: Actions on structure – Wind actions. *Technical Report*, European committee for standardization, Rue de Stassart, Brussels 1995.

Frank H. Extreme winds over Denmark from the NCEP/NCAR reanalysis. *Technical Report Risoe-R-1238(EN)*, Risø National Laboratory, Roskilde, Denmark, *http://www.risoe.dk/rispubl/VEA/ris-r-1238.htm* 2001.

Gumbel EJ. *Statistics of extremes*. Columbia University Press, 1958.

Hofherr T and M Kunz: Extreme wind climatology of winter storms in Germany, *Clim. Res*. 41, 105 – 123.
Kristensen et al. (2002): Sampling statistics of atmospheric observations. Wind Energy, 5, 301-313.

Kalnay E, Kanamitsu M, Kistler R, Collins W, Deaven D, Gandin L, Iredell M, Saha S, White G, Woollen J, *et al.* (1996) The NCEP/NCAR 40-year reanalysis project. *Bull. Am. Meteorol. Soc.* **77**: 437–471

Kunz M. et al. Assessment of extreme wind speeds from regional climate models – Part 1: Estimation of return values and their evaluation. Nat. Hazards Earth Syst. Sci. 10, 907 – 922.

Kwun JH, Kim Y, Seo J, Jeong J, You SH. Sensitivity of MM5 and WRF mesoscale model prediction of surface winds in a typhoon to planetary boundary layer parameterization. *Nat Hazards* 2009; **51**:63–77.

Landberg L, Myllerup L, Rathmann O, Petersen E, Jørgensen B, Badger J, Mortensen N. Wind resource estimation - An overview. *Wind Energy* 2003; **6**:261–271.

Larsén X, Mann J. Extreme winds from the NCEP/NCAR reanalysis data. *Wind Energy, DOI: 10.1002/we.318* 2009; **12**:556–573.

Larsén X, Mann J, Berg J, Göttel H, Jacob D. Wind climate from the regional climate model REMO. *Wind Energy, DOI: 10.1002/we.337* 2010; **13**:279–296.

Larsén X.G., Ott S., Badger J., Hahmann A.N. and Mann J. 2012a: Recipes for correcting the impact of effective mesoscale resolution on the estimation of extreme winds. Journal of applied meteorology and climatology, DOI: 10.1175/JAMC-D-11-090.1, vol. 51, p521 – 533.

(Earlier version of part of this work also appeared in EWEC 2011, in the scientific proceedings, p213 – 216.)

Larsén X.G., Badger J., Hahmann A.N. and Mortensen N.G. 2012b: The selective dynamical downscaling method for extreme wind atlases. Wind Energy, in press.
(Earlier version of part of this work also appeared in EWEC 2011, in the scientific proceedings, p186 – 189.)

Larsén X.G., Vincent C. and Larsen S.E. 2012c: The spectral structure of mesoscale winds over water. Q. J. R. Meteorol. Soc. In press.

Mann J, Kristensen L, Jensen NO. Uncertainties of extreme winds, spectra and coherences. *Bridge Aerodynamics, ISBN 9054109610*, Larsen, Esdahl (eds.). Rotterdam: Balkema, 1998.

Mann et al. 2000: WAsP Engineering, Technical report Risoe-R-1356(EN).

Mortensen N, Hansen J, Badger J, Jørgensen B, Hasager C, Youssef L, Said U, Moussa A, Mahmoud M, Yousef A, *et al.*. *Wind atlas for Egypt, measurements and modelling 1991 - 2005*. Risø National Laboratory, New and renewable energy authority, Cairo, Egypt and Egyptian meteorological authority, ISBN 87-550-3493-4, 2005.

Nielsen N, Sass B. A numerical, high resolution study of the life cycle of the severe storm over Denmark on 3 December 1999. *Tellus* 2003; **55**:338–351.

Peña A, Gryning S-E. Charnock's Roughness Length Model and Non-dimensionalWind Profiles Over the Sea. *Boundary Layer Meteorol.* **128**: 191-203

Pryor S, RJBarthelmie, Clausen N, Drews M, Mackeller N, Kjellström E. Analysis of possible changes in intense and extreme wind speeds over northern Europe under climate change scenarios. *Clim. Dyn.* 2010; doi:10.1007/s00382-010-0955-3.

Rogers A.L., Rogers J.W. and Manwell J.F., 2005, Comparison of the Performance of Four Measure-Correlate-Predict Algorithms, *J. Wind Eng. Ind. Aerodyn.* **93**: 243-264

Skamarock W, Klemp J, Dudhia J, Gill D, Barker D, Wang W, Powers J. A description of Advanced Research WRF. *Technical Report NCAR/TN-468+STR*, NCAR, NCAR, Boulder, Colorado, USA 2007.

Stathopoulos C., Barranger N., Larsén X. G. and Rodringo J. S. (2012): Implementation of spectrum analysis in the mesoscale modeling for wind energy assessment studies. 12th EMA/9th ECAC annual meeting Abstracts 9:EMS2012-282.

Weisse R, Storch H, Feser F. Northeast Atlantic and North Sea storminess as simulated by a regional climate model during 1958-2001 and comparisons with observations. *Journal of Climate* 2005; **18**:465–479.